Exergy and Economic Assessments of Solar Organic Rankine Cycle System with Linear V-Shape Cavity

E. Askari-Asli Ardeh[a*], Reyhaneh Loni[b], G. Najafi[b,], B. Ghobadian[b], Evangelos Bellos[c], D. Wen[d,e]**

[a] Department of Biosystems Engineering, University of Mohaghegh Ardabili, Ardabil, Iran.
[b] Department of Biosystems Engineering, Tarbiat Modares University, Tehran, Iran.
[c] Thermal Department, School of Mechanical Engineering, National Technical University of Athens, Greece.
[d] School of Aeronautic Science and Engineering, Beihang University, Beijing, China.
[e] School of Chemical and Process, Engineering University of Leeds, Leeds, UK

Corresponding Authors:ezzataskari@uma.ac.ir, g.najafi@modares.ac.ir

Abstract

In this research, a parabolic trough concentrator with linear V-Shape cavity receiver was studied as the heat source of an organic Rankine cycle system. The solar organic Rankine cycle system was evaluated under exergy and economic analyses. Thermal oil was used as the solar working fluid, and ethanol was used as the organic working fluid under different turbine inlet temperaturesand turbine inlet pressure. The influence of different operational parameters, including solar radiation, mass flow rate, and inlet temperature of solar working fluid was investigated on the performance of the solar organic Rankine cycle system. It was found that exergy gain and exergy efficiency of the solar system improved with increasingsolar radiation, increasinginlet temperature, and decreasingthe flow rate of the solar working fluid. The highest organic Rankine cycle efficiency and total efficiency were found to be 35%, and 25% at turbine inlet temperature of 592 K and turbine inlet pressureof 6 MPa, respectively. Finally, the lowest levelized cost of electricity, and the lowest payback period were calculated equal to 0.0716

(€/kWh), and 8.79 (years) for the optimum condition of the developed solar organic Rankine cycle system, respectively. The present study is beneficial for improving the performance of the solar organic Rankine cycle systems with parabolic trough concentrators in a simple and convenient way and the development of solar thermal technologies.

Keywords: Exergy and economic analyses; solar organic Rankine cycle system; parabolic trough concentrator; linear V-Shape cavity receiver.

Nomenclature

A	Area, m^2
c_p	Specific heat capacity, J/kgK
d_0	Cavity depth, m
d	Receiver tube diameter, m
Gr	Grasshof number
g	Gravity acceleration, m/s^2
h	Heat transfer coefficient, W/m^2K
I	Directnormalsolar irradiation, W/m^2
K	Thermal conductivity,W/mK
$\dot{m}$	System mass flow rate, kg/s
N	Number of tube sections
Nu	Nusselt number
P	Pressure, Pa
Pr	Prandtl number
$\dot{Q}_{net}$	Net heat transfer rate, W
$\dot{Q}^*$	Rate of available solar heat at the cavity receiver, W
$\dot{Q}_{loss}$	Loss rate of heat loss from the cavity receiver, W
$\dot{Q}_{solar}$	Rate of available solar heat at dish concentrator, W
R	Thermal resistance, K/W
Ra	Raleigh number
Re	Reynolds number
T	Temperature, K
t	Thickness, m
w	Wide, m

Greek symbols

α	Radiation absorptivity
ε	Emissivity
η	Efficiency
λ	Thermal conductivity, W/(m K)
ρ	Density, kg/m^3
σ	Stefan–Boltzmann constant, W/m^2K^4

Subscripts

a	air
ap	aperture
cavity	for the cavity
combined	combined convection
con	due to convection
ext	external
f	fluid
forced	due to forced convection
gc	glass cover
int	internal
inlet	at the inlet
ins	insulation
n	tube section number
natural	due to natural convection
net	net
PTC	parabolic trough concentrator
r	receiver
rad	due to radiation

s	surface of the inner tube	total	total
sun	sun	0	initial inlet to receiver
th	thermal	∞	infinitive

1 Introduction

Nowadays, renewable energies are accounted as an interesting source of energy for providing the social required energy [1]. There are different kinds of renewable energy, including solar, wind, geothermal, hydropower, etc. [2]. The solar energy is investigated as worldwide renewable energy that is accessible in different countries [3]. The solar energy can be converted to thermal energy using solar collectors. The solar collectors are divided two categories consist of concentrator and non-concentrator collectors [4]. There are different types of solar concentrator, including dish concentrator, Parabolic Trough Concentrator (PTC), linear Fresnel collector, and Compound Parabolic Concentrator (CPC). The PTCs are accounted as an interesting and industrial collector [5]. Generally, there are two types of absorber for the PTC collector, including evacuated tube receivers, and cavity receivers [6]. The cavity receivers are introduced as efficiently solar receiver for achieving the highest thermal energy in the solar concentrator collectors [7].

There are numerous studies related to the performance investigation of PTC collectors, numerically and experimentally [8]. Conrado et al. [9] presented a review paper related to numerical and experimental studies of PTC systems. Bellos and Tzivanidis [6] reviewed different design methods for PTC system. Chen et al. [10] experimentally invested performance of a PTC system. They found the efficiency of the solar system was estimated equal to 60% during winter. Lamrani et al. [11] numerically investigated a PTC system under variation of inlet temperature. They found the application of oil was more suitable compared to water as the solar working fluid. The thermal efficiency of the solar system was calculated by 76% during the summer. Moudakkar et al. [12] investigated the performance of a PTC system as the heat source of a dryer. They developed two models based on uniform and non-uniform distribution of heat flux. Both investigated model showed good agreement compared to measured experimental results. Fathy et al. [13] experimentally considered the performance of a desalination system with PTC as the heat source. They found the performance of the desalination system had higher amounts with PTC compared to conventional desalination system. Razmmand et al. [14] evaluated the performance of a PTC system with application of nanofluids as heat transfer fluid. They found the performance of the solar system improved using nanofluid as the solar working fluid.

Rehan et al. [15] experimentally tested the performance of a low concentration PTC with the application of nanofluids. Various nanofluids in different concentrations and flow rates were considered. Alumina/water nanofluid showed higher performance compared to Fe_2O_3/water nanofluid as the solar working fluid. Potenza et al. [16] experimentally tested application of CuO/air nanofluid as the solar working fluid of a PTC system. The thermal efficiency of the system was measured equal to 65% using nanofluid. Bellos et al. [17] investigated improvement methods of PTC efficiency utilizing the application of nanofluids and turbulators. They reported an efficiency improvement of 1.54% using a combination of two suggested methods for improving PTC performance.

As mentioned, cavity receivers are investigated as an effective way of improving the performance of solar concentrating systems [18]. Some researches considered the application of cavity receivers as absorbers of the dish concentrators [19]. Loni et al. [20] numerically and experimentally investigated the effect of wind on the performance of a dish concentrator with a hemispherical cavity receiver. They suggested some experimental relationship for prediction of wind effect on the performance of the hemispherical cavity receiver. In another research, Loni and his colleagues [21] numerically and experimentally evaluated the thermal performance of a dish concentrator with two shapes of cavity receiver, including cylindrical and cubical cavity receivers. Also, some researches were done the related application of linear cavity receiver in solar linear concentrators such as the linear Fresnel collector, and PTC systems [22]. Qiu et al. [23] investigated the optical and thermal performance of a linear Fresnel concentrator with a trapezoidal cavity receiver. Xiao et al. [24] evaluated the performance of a PTC system with a new shape of the linear cavity receiver. They found the performance of the solar system can be improved using internal fins.

On the other hand, Organic Rankine Cycles (ORCs) are introduced as an important thermodynamic cycle for power generation from the low-temperature heat source, including solar energy [25]. Some researchers numerically have studied the performance of the ORC systems with the solar PTC collector as the ORC heat source [26]. On the other hand, some researchers have investigated solar systems based on financial aspects [27]. Bellos and Tzivanidis [3] studied a solar power generation system financially. Two kinds of the solar linear concentrator, including parabolic trough concentrator and linear Fresnel concentrator, were investigated. They found the parabolic trough concentrator can be introduced as a more useful collector for absorbing energy. In another work, Bellos et al. [28] investigated a solar-driven absorption chiller under energy, exergy and economic aspects. Optimum parameters of the solar system and storage tank were reported. Najafi et al. [29] thermos-economically evaluated a solar-conventional energy supply system. They investigated a direct absorption PTC collector. They assessed the solar system for different weather conditions.

As seen from the literature as mentioned above, there is no reported paper related to performance investigation of a solar ORC system with linear V-Shape cavity receiver as an absorber of a PTC system. In this research, a PTC system using a linear V-Shape cavity receiver was investigated as the heat source of an ORC system under energy and economic analyses as a novelty subject. Influence of different operational parameters including solar radiation, mass flow rate, and inlet temperature of working fluid as well as parameters of the ORC system including different TITs were investigated on the performance of the solar ORC system. Results of this research can be used for designing an ORC system with the highest performance and lowest cost. The examined novel PTC is a cost-effective technology because it has not evacuated tube, which is an expensive device. Moreover, it presents higher reliability compared to the conventional systems because there is not the danger of losing the vacuum.

2 Modelling and Description

In this research, the performance of a solar ORC system with a PTC system was numerically investigated. A linear V-Shape cavity receiver was used as the ORC heat source. A schematic of the investigated solar ORC system with the linear V-Shape cavity receiver is presented in Figure 1. Thermal oil was used as the solar working fluid, whereas different organic fluids were investigated as the ORC working fluid. The ORC system consisted of a heat exchanger (evaporator), turbine, condenser, and pump. Absorbed thermal energy by the solar collector transferred to the ORC system by the heat exchanger. It should be mentioned that the turbine produced power, the condenser ejected thermal energy, and the pump circulated the ORC working fluid. As seen from Figure 1, absorbed solar energy by flowing thermal oil in the linear V-Shape cavity receiver was transferred to the ORC working fluid using the heat exchanger.

Generally, power was produced by flowing the high-temperature and high-pressure ORC working fluid in the turbine.

Generally, there are two types of solar collector parameters, including structural, and operational factors that influence the performance of the solar and ORC system. The structural parameters are including PTC aperture area, cavity aperture area, cavity height, etc. About operational parameters, they are including inlet temperature, and flow rate of the solar working fluid, types of the solar working fluid, etc. Additional to these parameters, environmental factors are an influence on the performance of the solar PTC and ORC system, including ambient temperature, wind speed, and solar radiation, too.

It should be mentioned that variation of the solar system parameters influences the performance of the ORC system because of using the absorbed heat by the solar system as a heat source of the ORC system. On the other hand, some parameters of the ORC systems influence the performance of the ORC system, too. These parameters are including turbine inlet pressure, turbine inlet temperature, condenser temperature, type of ORC working fluid. In this study, the influence of solar radiation, the inlet temperature of the solar working fluid, and the flow rate of solar working fluid was investigated on the performance of the solar ORC system. Also, the influence of turbine inlet temperature on the ORC performance was investigated.

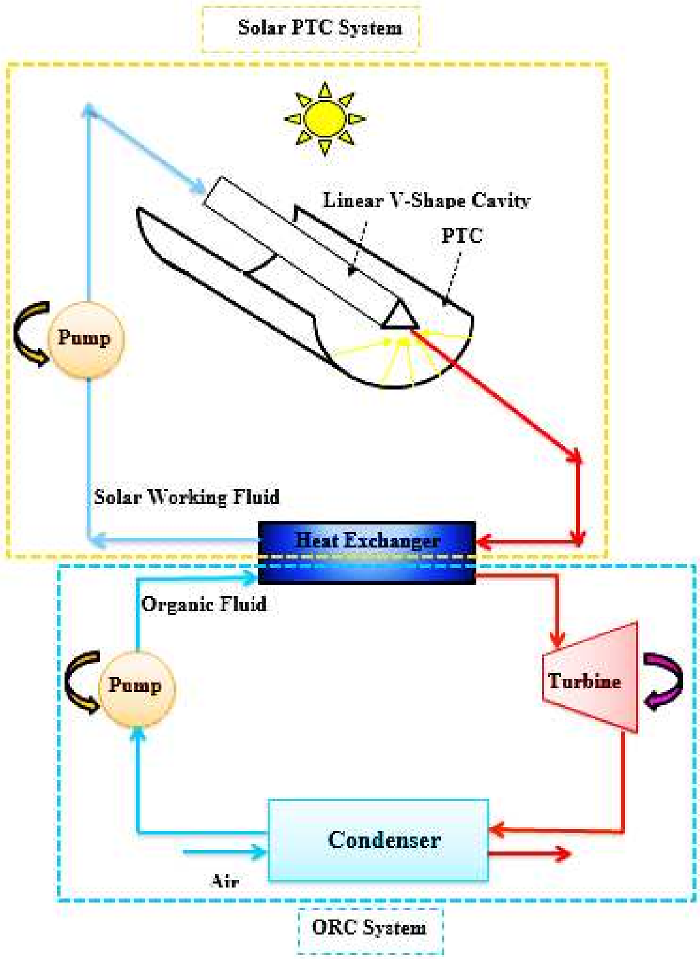

Figure 1: A schematic of the solar ORC system with linear V-Shape cavity receiver as ORC heat source.

In this research, the solar PTC system was investigated as the ORC heat source with ethanol as the ORC working fluid. Finally, the solar ORC system was economically evaluated for power generation. Analysis processes of the current research are depicted in Figure 2. All of these analyses were presented in detail in the next sections.

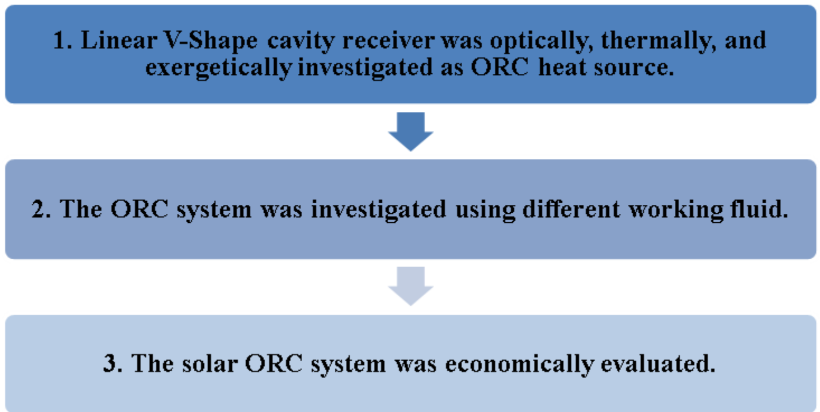

Figure 2: Analysis process of the current research.

2.1 Solar Parabolic Trough Concentrator Modeling

Optical analysis of the solar PTC system with linear V-Shape cavity receiver was conducted using SolTrace software. The SolTrace software is introduced as free and effective software for optical modelling of solar concentrating systems [30, 31]. A view of the linear V-Shape cavity receiver is presented in Figure 3. The solar PTC system was simulated with sun shape as a pillbox, half-angle width as 4.65 mrad, number of ray intersections as 10000, optical error as 10 mrad, and tracking error as 1º. Structural parameters of the solar PTC system during the optical and thermal modelling are reported in

Table 1. A view of the solar system elements is presented in Figure 4.

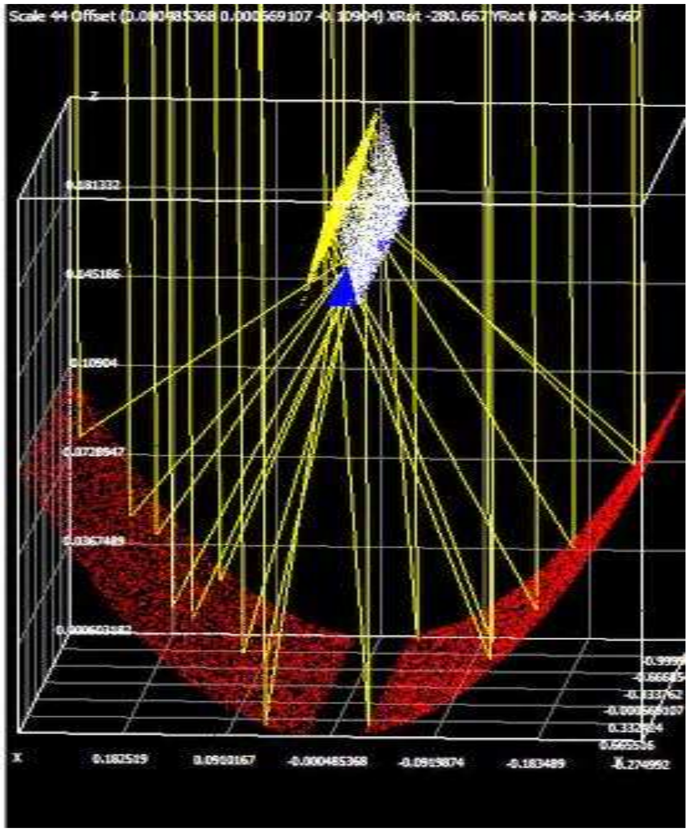

Figure 3: A view of the optical analysis by SolTrace software.

Table 1: Structural parameters of the solar PTC system.

Description	Dimension
Parabola length	2 m
Parabola aperture	50 cm
Focal distance	17.5 cm
Cavity aperture width	5 cm
Cavity length	2 m
Cavity angle	60º
Cavity coating absorbance coefficient	0.85

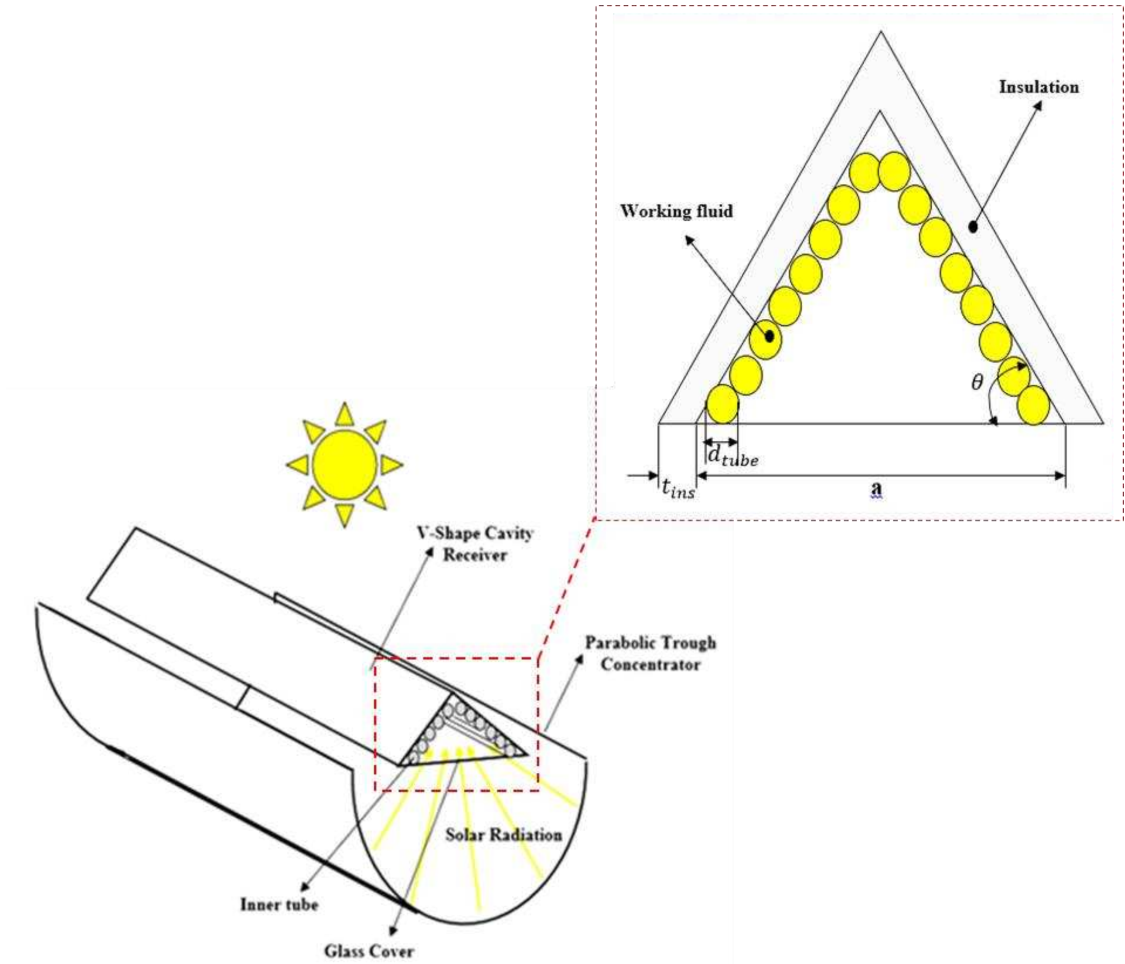

Figure 4: A view of the solar system elements.

Thermal modelling of the solar PTC system was numerically done based on energy balance equations and thermal resistance method. The energy balance equations were developed in Maple software. Thermal heat losses from the linear V-Shape cavity receiver include conduction, radiation, and convection heat losses. A schematic of the heat losses from the V-Shape cavity receiver is depicted in Figure 5. As mentioned, the thermal resistance method was used for thermal modelling of the investigated solar PTC system. A view of the thermal resistance method that used for thermal modelling of the linear V-Shape cavity receiver is presented in Figure 6. All of the mentioned thermal resistance in Figure 6 has been shown in Appendix A.

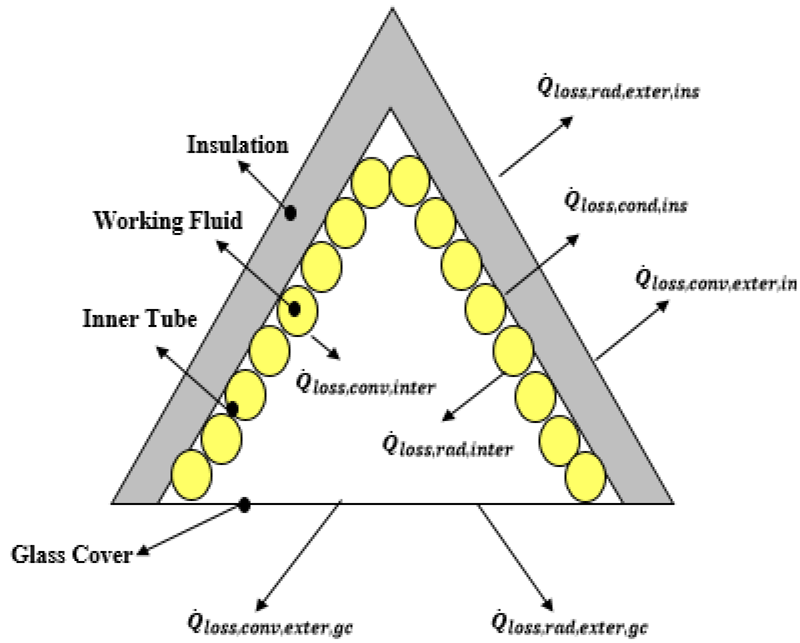

Figure 5: A schematic of the investigated linear V-Shape cavity receiver.

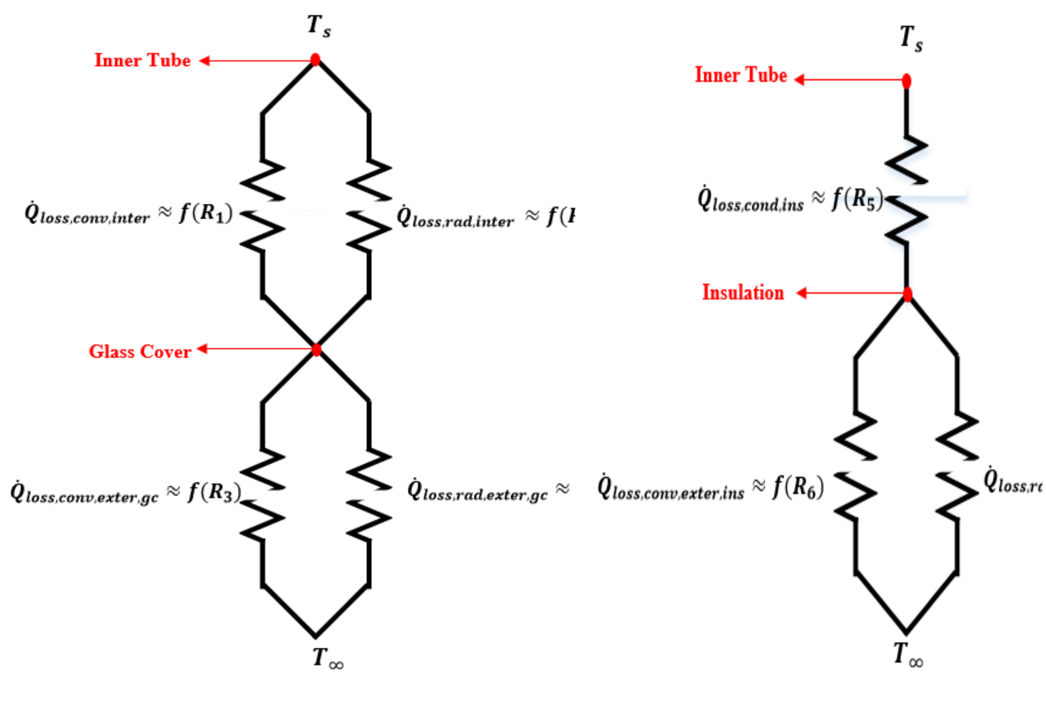

(a) **(b)**

Figure 6: Schematic of used thermal resistance method for a) internal heat losses, and b) external heat losses from the V-Shape cavity receiver.

The cavity tube was divided to smaller lengths along the cavity tube for calculating accuracy results. Solar heat flux on each element of the cavity tube was calculated using the SolTrace software. Heat gain ($\dot{Q}_{net,n}$), and cavity surface temperature ($T_{s,n}$) of each element were calculated using the following equations [32]:

$$\dot{Q}_{net,n} = \frac{\left(T_{s,n} - \sum_{i=1}^{n-1}\left(\frac{\dot{Q}_{net,i}}{\dot{m}c_{p0}}\right) - T_{inlet,0}\right)}{\left(\frac{1}{h A_n} + \frac{1}{2\,\dot{m}c_{p0}}\right)} \quad \textbf{(1)}$$

And

$$\dot{Q}_{net,n} = \dot{Q}^{*}{}_{n} - \frac{A_n}{R_{total}}\left(T_{s,n} - T_{\infty}\right) \quad \textbf{(2)}$$

It should be mentioned, internal convection heat transfer of the working fluid in the cavity tube is calculated based on Eq. **(1)**, whereas external heat transfer from the cavity tube is assumed using **(2)**. Finally, the thermal efficiency of the solar PTC system can be calculated as following [32]:

$$\eta_{th} = \frac{\dot{Q}_{net}}{\dot{Q}_{solar}} = \frac{\sum_{1}^{N}\dot{Q}_{net,n}}{\dot{Q}_{solar}} \quad \textbf{(3)}$$

Where

$$\dot{Q}_{solar} = I_{sun}A_{ap,PTC} \quad \textbf{(4)}$$

In these equations, $\dot{Q}_{net}$(W) shows total absorbed heat by the solar working fluid, and $\dot{Q}_{solar}$(W) presents total received solar energy by the solar PTC collector. It should be mentioned, Behran thermal oil with the following thermal properties was used as the solar working fluid[33]:

$$k_f = 0.1882 - 8.304 \times 10^{-5}(T_f) \qquad (\frac{W}{mK}) \tag{5}$$

$$c_{p,f} = 0.8132 + 3.706 \times 10^{-3}(T_f) \qquad (\frac{kJ}{kgK}) \tag{6}$$

$$\rho_f = 1071.76 - 0.72(T_f) \qquad (\frac{kg}{m^3}) \tag{7}$$

$$Pr = 6.73899 \times 10^{21}(T_f)^{-7.7127} \tag{8}$$

In these equations, T_f (K) is working fluid temperature, k_f ($\frac{W}{mK}$) is working fluid conductivity, $c_{p,f}$ ($\frac{kJ}{kgK}$) is special heat capacity of the working fluid, ρ_f ($\frac{kg}{m^3}$) working fluid density, and Pr is Prandtl number of the working fluid.

2.2 Exergy Analyses

Exergy is a tool for prediction of the maximum available useful work during a process that brings the system into equilibrium with environmental. Exergy efficiency of the system can be defined as cavity receiver exergy rate to rate of solar exergy as following [34]:

$$\eta_{th,ex} = \frac{\dot{E}_{gain}}{Ex_{Sun}} \tag{9}$$

In this equation, $\dot{E}_{gain}$ (W) is the exergy rate of the cavity receiver that can be calculated as below [34]:

$$\dot{E}_{gain} = \dot{m} \cdot C_p \cdot \left(T_{outlet} - T_{inlet} - T_{amb} \ln\left(\frac{T_{outlet}}{T_{inlet}}\right)\right) - \frac{T_{amb}}{T_f}\frac{\dot{m}\,\Delta P}{\rho} \tag{10}$$

And, Ex_{Sun}(W) is exergy delivery by the sun that can be estimated using the following equation [34]:

$$Ex_{Sun} = I_{sun}A_{aperture,PTC}\left[1 - \frac{4}{3}\cdot\frac{T_{amb}}{T_{sun}} + \frac{1}{3}\left(\frac{T_{amb}}{T_{sun}}\right)^4\right] \tag{11}$$

In this equation, T_{sun} is assumed equal to 5762 K. Pressure drop of the solar working fluid in the cavity receiver can be defined as following [32]:

$$\Delta P = \frac{\rho\cdot\left({V^2}_{Avg}\right)}{2}\cdot(f_r\cdot\frac{L}{d} + \sum_y K_y) \tag{12}$$

$$\Delta P = \frac{8\cdot\dot{m}^2}{\rho\cdot\pi^2\cdot d^4}\cdot(f_r\cdot\frac{L}{d} + \sum_y K_y) \tag{13}$$

Moreover, the equivalent thermal output ($\dot{Q}_{eq}$) is defined as follows:

$$\dot{W}_{Pump} = \frac{\Delta P\cdot\dot{m}}{\rho} \tag{14}$$

$$\dot{Q}_{eq} = (\dot{Q}_{net} - \frac{\dot{W}_{Pump}}{\eta_{el}}) \tag{15}$$

Where η_{el} will be assumed equal to 0.33 for the investigated system. This value is practically the mean electrical efficiency of the grid. The overall efficiency is defined using the equivalent thermal output and the solar energy input:

$$\eta_{overall} = \frac{\dot{Q}_{eq}}{\dot{Q}_{solar}} \tag{16}$$

2.3 Organic Rankine Cycle System Modeling

As mentioned previous, the solar PTC system with the linear V-Shape cavity receiver was investigated as the ORC heat source. Ethanol was used as the ORC working fluid. The ORC system was evaluated under variation of turbine inlet temperature (TIT), and turbine inlet pressure (TIP). A schematic of the entropy-temperature graph of the ORC system with Ethanol as the working fluid is presented in Figure 7.

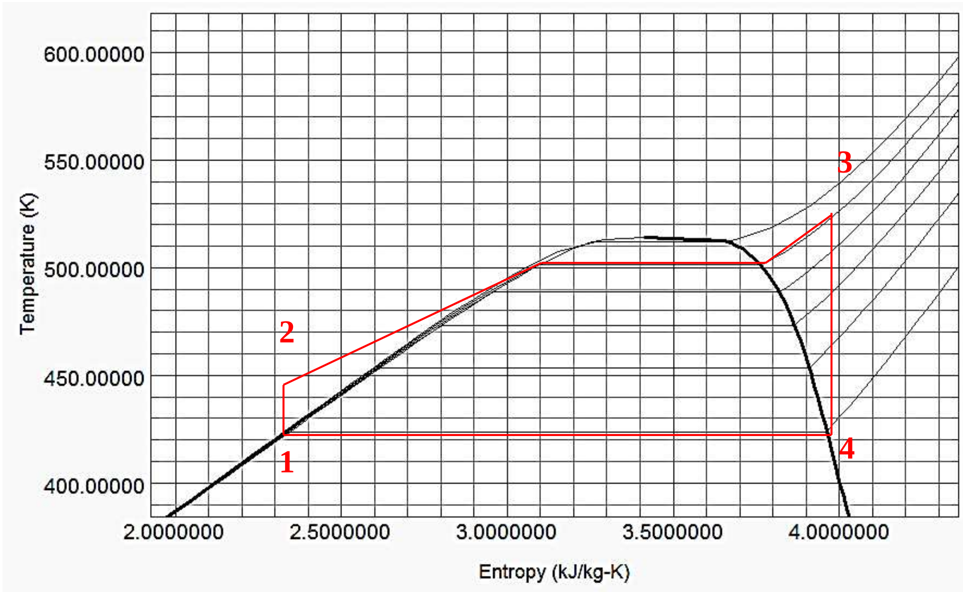

Figure 7: A schematic of the entropy-temperature graph of the ORC system with Ethanol as the working fluid.

In this research, it was assumed that absorbed solar energy by the solar system was used as the heat source of the ORC system. Consequently, the mass flow rate of the ORC working fluid can be calculated as following [34]:

$$\dot{m}_{ORC} = \frac{\dot{Q}_{evp}}{(h^*{}_3 - h^*{}_2)} \quad \textbf{(17)}$$

In this equation, $\dot{Q}_{evp}$ (W) is equal to the cavity heat gain, $h^*{}_2$ (kJ/kg) is the enthalpy at the evaporator inlet and $h^*{}_3$(kJ/kg) is the enthalpy at the evaporator outlet.

On the other side, the generated power by the turbine can be estimated as below [34]:

$$\dot{W}_T = \dot{m}_{ORC}(h^*{}_3 - h^*{}_4) \quad \textbf{(18)}$$

In this equation, $h^*{}_3$ (kJ/kg), and $h^*{}_4$(kJ/kg) are the enthalpy at the turbine inlet and the turbine outlet, respectively. Also, the rejected heat in the condenser can be estimated using the following equation [34]:

$$\dot{Q}_c = \dot{m}_{ORC}(h^*{}_4 - h^*{}_1) \tag{19}$$

In this equation, $h^*{}_4, and\ h^*{}_1$ (kJ/kg) are the enthalpy at the condenser inlet and the outlet, respectively.

Finally, the consumed power in the pump is calculated by the following equation [34]:

$$\dot{W}_P = \dot{m}_{ORC}(h^*{}_2 - h^*{}_1) \tag{20}$$

The net power of the ORC system is calculated as:

$$\dot{W}_{net} = \dot{W}_T - \dot{W}_P = \dot{m}_{ORC}[(h^*{}_3 - h^*{}_4) - (h^*{}_2 - h^*{}_1)] \tag{21}$$

ORC efficiency can be defined as follows:

$$\eta_{ORC} = \dot{W}_{net} / \dot{Q}_{evp} \tag{22}$$

On the other side, overall solar ORC efficiency can be evaluated as below:

$$\eta_{overall} = \dot{W}_{net} / (I_{beam}.A_{PTC}) \tag{23}$$

The ORC system was evaluated under variation of TIP between 1 MPa to 6 MPa, condenser temperature as 311 K, and the ambient temperature of 301 K.

2.4 Economic Analyses

In this study, the developed solar ORC system was economically investigated. One of the investigated economic parameters is Levelized Cost of Electricity (LCOE) that can be defined as the investment and maintenance cost of the solar ORC system during the lifetime as (€) to the generated power by the solar ORC system as kWh. The LCOE can be calculated as the following equation:

$$LCOE = \frac{I_t + M_t + F_t}{E_t} \tag{24}$$

Where I_t (€) is investment cost, M_t (€) is maintenance cost, F_t (€) is the cost of fossil fuel that is assumed equal to zero in this study, and E_t(kWh) is generated power. The investment cost of the solar ORC system can be calculated as follows:

$$I_t = I_{t,PTC} + I_{t,ORC} \tag{25}$$

In this equation, $I_{t,PTC}$ is the investment cost of the solar PTC system that was assumed from 200€/m^{2}for large scale setup, to 300 €/m^2 for small scale setup [3], and $I_{t,ORC}$ is the investment cost of the ORC system that was assumed from 2000€/kWh for large scale setup, to 4000 €/kWh for small scale setup[3]. Related to the maintenance cost of the solar ORC system, the below equation can be presented:

$$M_t = 0.01 \cdot N \cdot \ I_t \tag{26}$$

Where, N is the estimated lifetime of the solar ORC system that was assumed equal to 25 years in this research, and I_t was the investment cost of the solar ORC system that was calculated based on the previous equations. Finally, generated power, E_t(kWh), can be calculated as follows:

$$E_t = N \cdot \ E_{t,yearly} \tag{27}$$

Where $E_{t,yearly}$ (kWh) is yearly generated power by the solar ORC system, and N is the estimated lifetime of the solar ORC system that was assumed equal to 25 years in this research.

Another parameter for economic analysis is cash flow. The cash flow as the annual income minus maintenance costs can be calculated as follows:

$$CF = \left[E_{t,yearly} * C_{el}\right] - M_t \tag{28}$$

In this equation, CF (€) is the cash flow, C_{el} (€/kWh) is the financial value of electricity produced, which was assumed equal to 0.2 in this study [3].

Finally, Simple Payback Period (SPP) is another important parameter for economic analysis of a system. The SPP is defined as how long it takes for the system to be profitable. The SPP can be calculated as follows:

$$SPP = \frac{I_t}{CF} \tag{29}$$

2.5 Validation of the Developed Model

The developed system was validated based on the reported experimental data by [35]. A view of the experimental setup is presented in Figure 8. Figure 9 shows the variation of thermal efficiency versus variation of $\left(\frac{T_f - T_{amb}}{I_{beam}}\right)$ for the reported experimental results and numerical results based on the current research. As seen, there is a good agreement between the measured experimental results and calculated numerical results in this research. More specifically, the mean deviation between the numerical and the experimental results is about 1%, which is a relatively low value.

Figure 8: Investigated the PTC system by ref. [35].

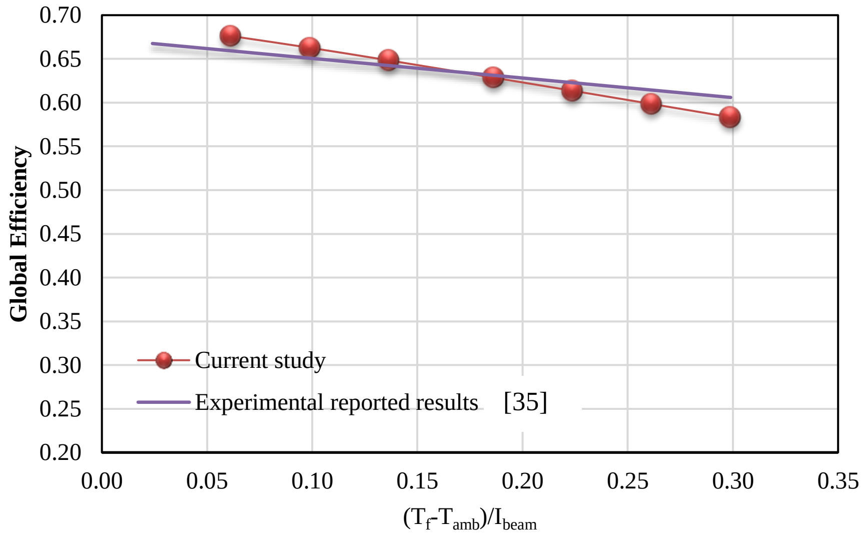

Figure 9: Comparison between the reported experimental results [35] and calculated results in this study.

3 Results and Discussion

In this section, results of the investigated solar ORC system with application of the linear V-Shape cavity receiver will be presented as follows:

- Firstly, exergy performance of the solar PTC with the linear V-Shape cavity receiver will be reported.
- Afterwards, the performance of the solar ORC system with the PTC collector to deliver heat to the ORC system will be presented.
- Finally, economic analyses of the suggested solar ORC system for power generation will be reported.

3.1 Exergy Analysis

In this section, the performance of the solar PTC with the linear V-Shape cavity receiver was investigated under exergy analysis. The cavity tube diameter was equal to 25 mm. Thermal oil was used as the solar working fluid. Influence of solar radiation, inlet temperature, and flow rate of the thermal oil was studied on exergy performance of the solar system. Figure 10a, 10b, and 10c display variation of exergy gain versus variation of solar radiation, inlet temperature, and flow rate of thermal oil, respectively. In Figure 10a, solar radiation changed in the range of 600 W/m^2 to 1100 W/m^2, and the inlet temperature and flow rate of the solar working fluid were assumed as constant amounts of 50℃, and 50 ml/s, respectively. As seen in Figure 10a, exergy gain of the solar system has increased with increasing solar radiation. Similar results have been reported in Ref. [36]. About Figure 10b, the inlet temperature of the solar working fluid was changed from 50℃ to 240℃. On the other side, the solar radiation, and the flow rate of the working fluid were investigated at constant amounts of 800 W/m^2, and 50 ml/s, respectively. It would be resulted from Figure 10b, exergy gain of the solar system enhanced with increasing inlet temperature of the solar working fluid. Similar results had been reported in Ref. [37]. Also, Figure 10c was depicted based on the flow rate of the solar working fluid in the range of 5 ml/s to 610 ml/s, and the solar radiation and inlet temperature of the working fluid equal to 800 W/m^2, and 50 ℃, respectively. As depicted in Figure 10c, higher amounts of the flow rate of solar working fluid resulted in lower amounts of the exergy gain.Similar conclusions have been reported in Ref. [37].Finally, it can be concluded that the exergy gain of the solar system improved with increasing solar radiation, increasing the inlet temperature of the solar working fluid, and decreasing the flow rate of the solar working fluid. It can be seen from Figure 10, the most effective parameter on the exergy gain of the solar PTC system with the V-shape cavity receiver is the inlet temperature of the heat transfer fluid. The exergy gain of the examined solar system improved up to nearly 220 W with an inlet temperature of the heat transfer fluid equal to 240 ºC as a new finding of the current research.

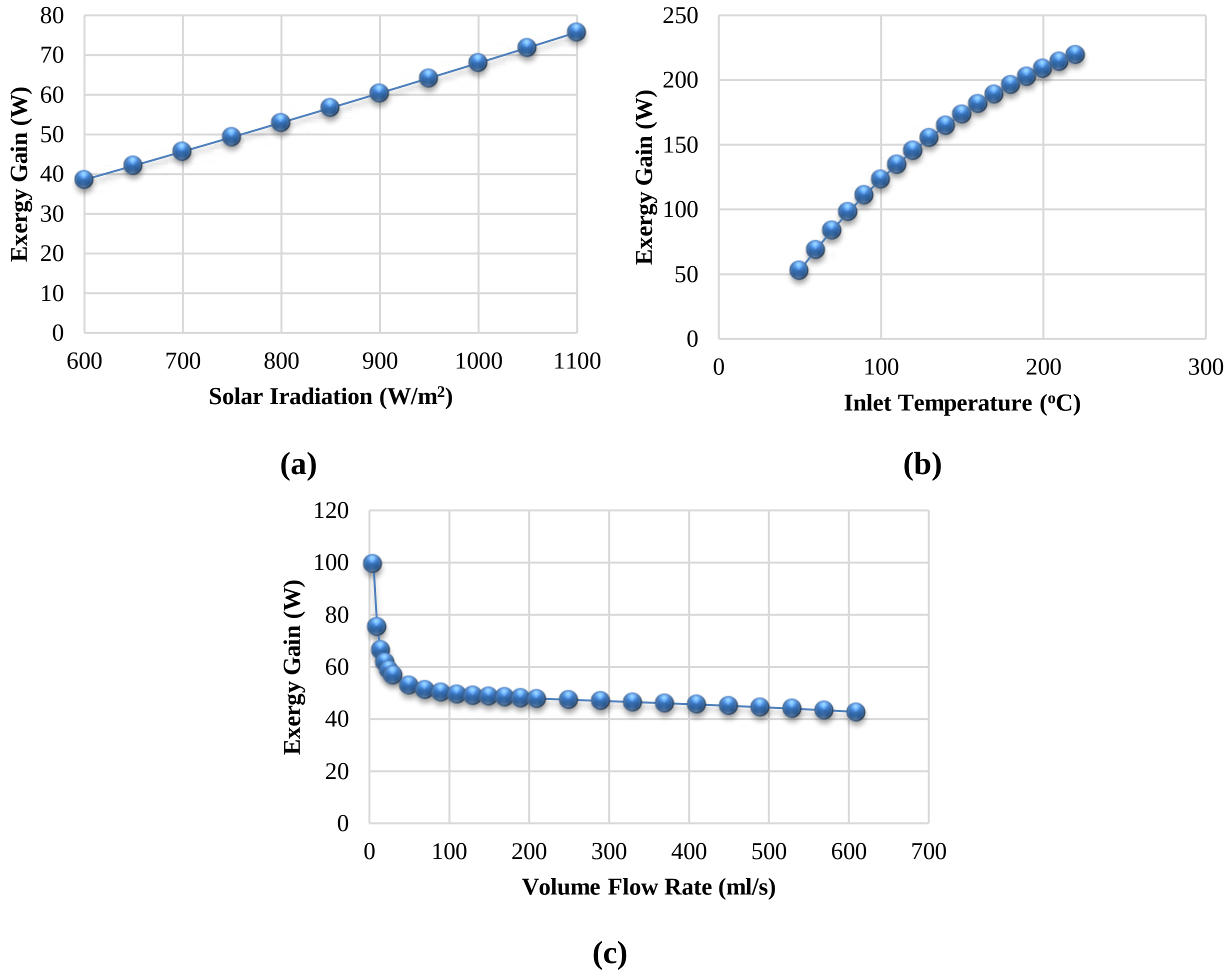

Figure 10: Variation of the collector exergy gain under variation of a) solar radiation, b) inlet temperature of thermal oil, and c) flow rate of thermal oil.

Variation of exergy efficiency of the solar PTC system versus variation of solar radiation, inlet temperature, and flow rate of thermal oil was depicted in Figure 11a, 11b, and 11c, respectively. It should be mentioned that the linear V-Shape cavity receiver with a tube diameter of 25 mm was used as the PTC absorber. Also, thermal oil was used as the solar working fluid. The solar radiation was varied between 600 W/m^2 to 1100 W/m^2 in Figure 11a. Also, amounts of the inlet temperature and flow rate of the solar working fluid were assumed equal to 50℃, and 50 ml/s in Figure 11a, respectively. As resulted from Figure 11a, the exergy efficiency of the solar system revealed higher amounts with increasing solar radiation amount. Similar results have been reported by other researches such as Refs. [36, 38].Related to Figure 11b, the inlet temperature of the solar working fluid was varied in the range of 50℃ to 240℃. And, the solar radiation and flow rate of the working fluid was investigated as a constant amount of 800 W/m^2, and 50 ml/s, respectively. As seen in Figure 11b, the exergy efficiency of the solar PTC system with V-Shape cavity receiver improved with increasing inlet temperature of the solar working fluid. Similar conclusions have been reported in Ref. [37].About Figure 11c, the flow rate of the solar working fluid was investigated between 5 ml/s to 610 ml/s, and the solar radiation and inlet temperature of the working fluid was assumed equal to 800 W/m^2, and 50 ℃, respectively. As resulted from Figure 11c, the exergy efficiency of the solar ORC system decreased with increasing the flow rate of the solar working fluid. Similar results had been reported in Ref. [37]. Consequently, higher amounts of the exergy efficiency of the solar system can be resulted in increasing solar radiation, increasing the inlet temperature of the solar working fluid, and decreasing the flow rate of the solar working fluid. Also, it can be seen that the exergy efficiency of the solar system has shown a similar trend compared to the variation of the exergy gain in the same condition. Similar to concluded results of the exergy gain, it could result from Figure 11, the most effective parameter on exergy efficiency of the solar PTC system with the V-shape cavity receiver is inlet temperature of the heat transfer fluid. The highest exergy efficiency of the solar system was calculated nearly 25% with an inlet temperature of 240 ºC as a new finding of the current study.

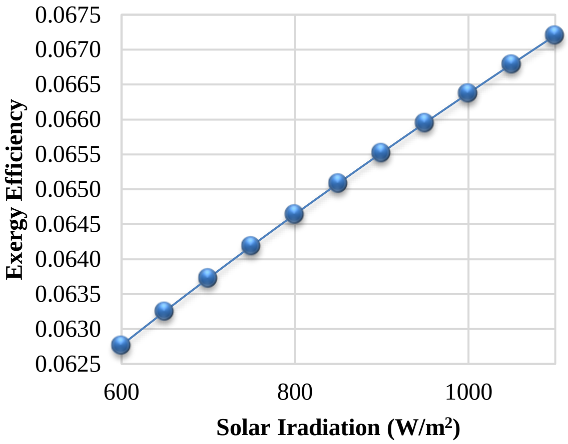

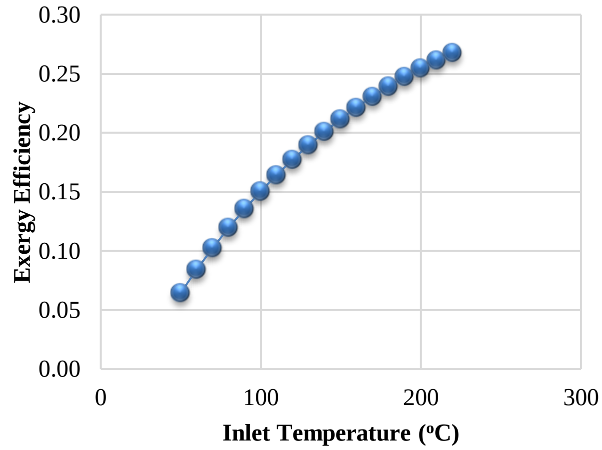

(a) **(b)**

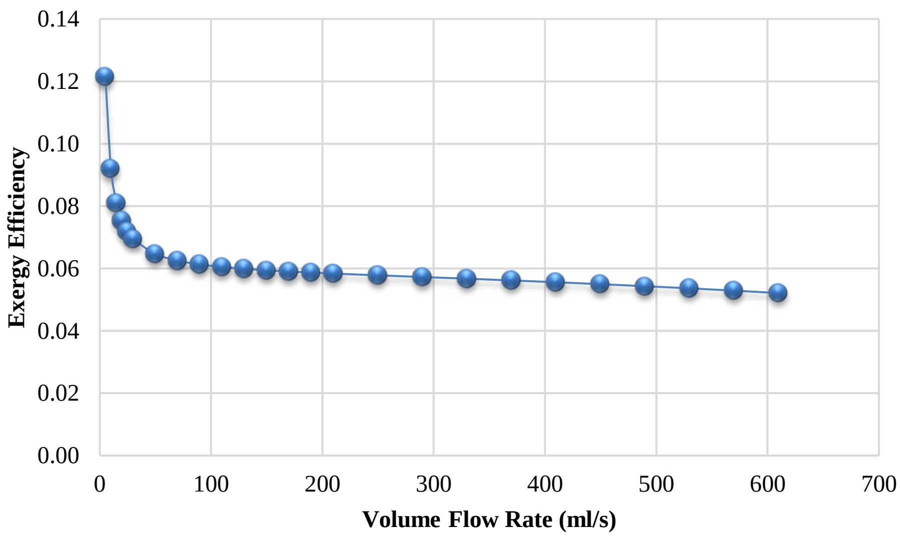

(c)

Figure 11: Variation of the collector exergy efficiency under variation of a) solar radiation, b) inlet temperature of thermal oil, and c) flow rate of thermal oil.

Figure 12a, 12b, and 12c depict the variation of cavity heat gain versus a change of solar radiation, inlet temperature, and flow rate of thermal oil, respectively. As mentioned, the linear V-Shape cavity receiver was used as the PTC receiver with a tube diameter of 25 mm. Thermal oil was used as the solar working fluid. Figure 12a has been reported for variation of the solar radiation between 600 W/m^2 to 1100 W/m^2. Also, amounts of the inlet temperature and flow rate of the solar working fluid were assumed constant equal to 50℃, and 50 ml/s during the analyses in Figure 12a, respectively. It can be seen in Figure 12a, the cavity heat gain increased with increasing solar radiation amount. On the other side, the inlet temperature of the solar working fluid was changed in the range of 50℃ to 240 ℃ in Figure 12b.Also, the solar radiation and flow rate of the working fluid wasassumedas 800 W/m^2, and 50 ml/s, respectively. It could be concluded from Figure 12b, the cavity heat gain decreased with increasing inlet temperature of the working fluid.A similar trend of data had been reported in Ref. [37]. Related to Figure 12c, the cavity heat gain was investigated with the variation of flow rate between 5 ml/s to 610 ml/s, the solar radiation equal to 800 W/m^2, and inlet temperature as of the 50 ℃. It could be resulted from Figure 12c, the cavity heat gain improved with an increasing flow rate of the solar working fluid. Similar results had been reported in Ref. [37]. It should be mentioned that the cavity heat gain had shown sharply increasing with an increasing flow rate of the solar working fluid until 100 ml/s and after that, the cavity heat gain has remained at an almost constant amount. Consequently, the optimum amount of flow rate equal to 100 ml/s could be defined for achieving the highest performance with the lowest power consumption.

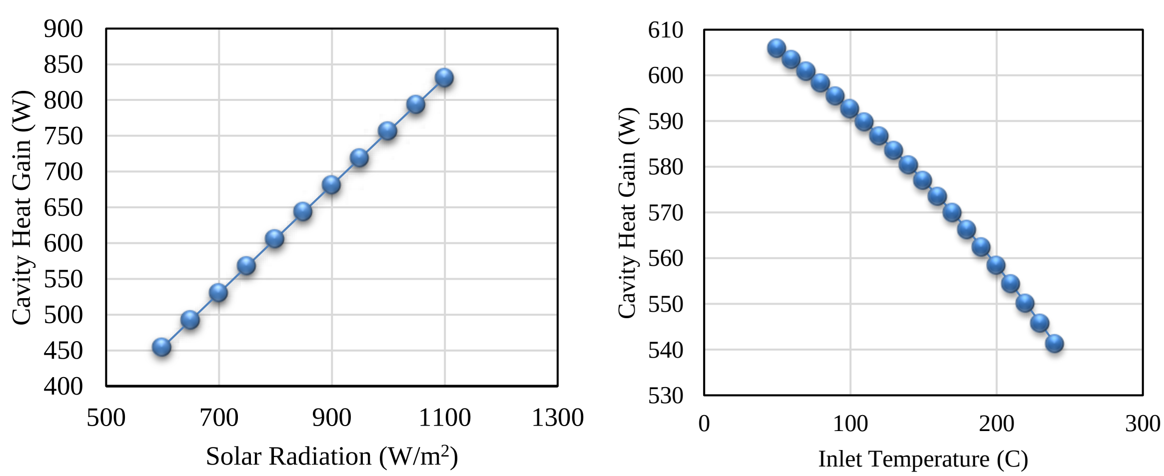

(a) **(b)**

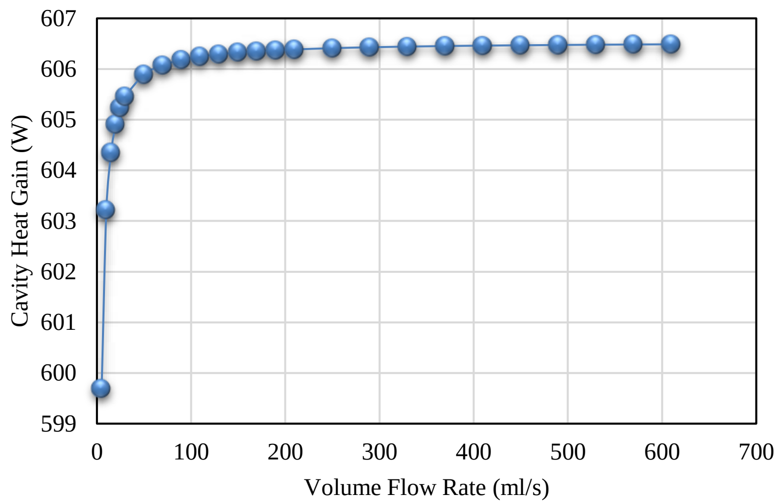

(c)

Figure 12: Variation of cavity heat gain under variation of a) solar radiation, b) inlet temperature of thermal oil, and c) flow rate of thermal oil.

Figure 13a, 13 b, and 13c show variation of outlet temperature of the solar working with changes in solar radiation, inlet temperature, and flow rate of thermal oil, respectively. The PTC collector with the linear V-Shape cavity receiver was studied. As mentioned, thermal oil was used as the solar working fluid. In these analyses, the solar radiation varied from 600 W/m^2 to 1100 W/m^2, the solar working fluid changed in the range of 50℃ to 240℃, and the flow rate of the solar working fluid was investigated between 5 ml/s to 610 ml/s in Figure 13a, 13b, and 13c, respectively. Whereas, default values of solar radiation of 800 W/m^2, the inlet temperature of 50℃, anda flow rate of 50 ml/s were assumed during the analyses. In Figure 13, the outlet temperature of the solar working fluid increased with increasing solar radiation, the inlet temperature of the working fluid, and decreasing flow rate of the solar working fluid. Similar results had been reported in Ref. [37].

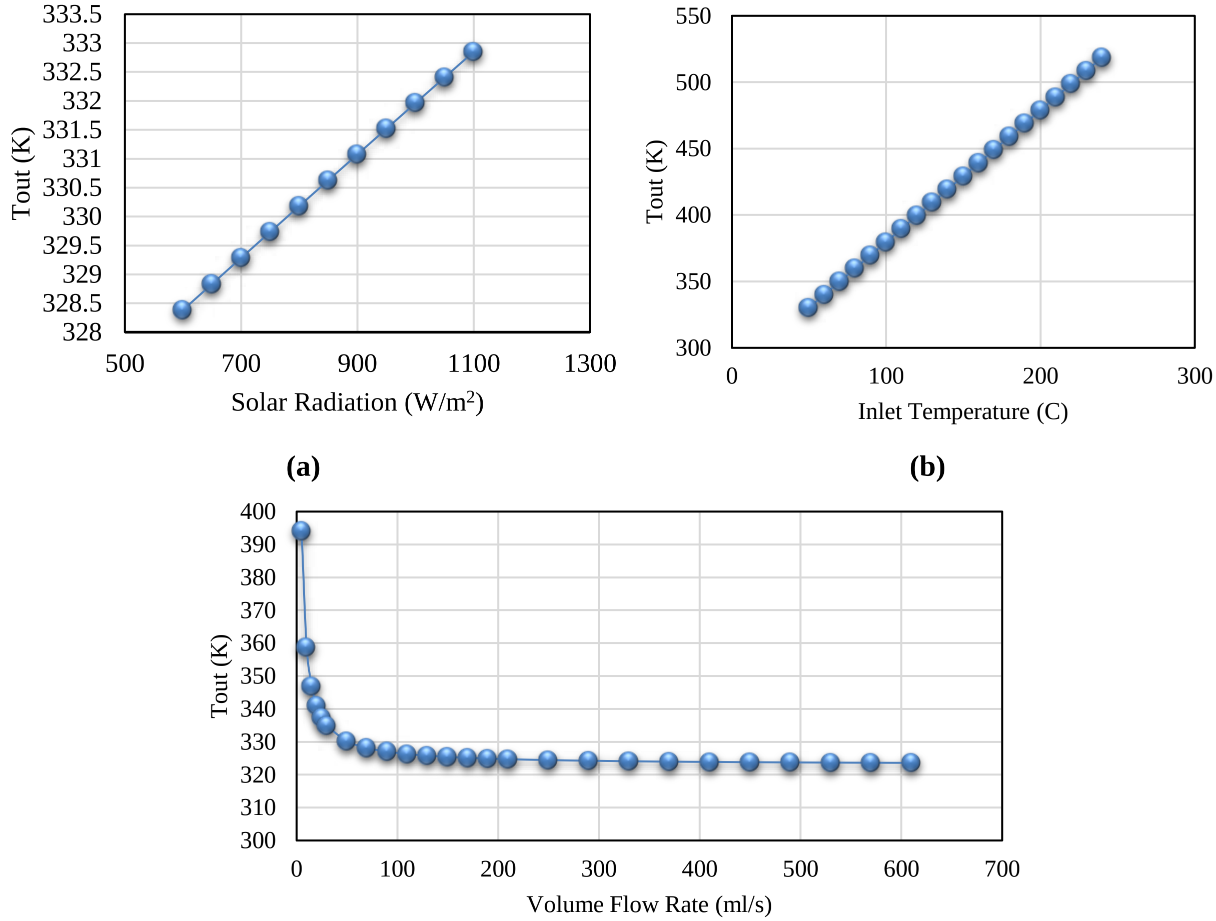

(c)

Figure 13: Variation of outlet temperature of solar working fluid under variation of a) solar radiation, b) inlet temperature of thermal oil and c) flow rate of thermal oil.

3.2 Solar Organic Rankine Cycle System

In this section, the performance of the solar ORC system with the PTC collector as the ORC heat source was investigated. The V-Shape cavity receiver was used as the PTC absorber, and thermal oil was studied as the solar working fluid. It should be mentioned that Ethanol was investigated as the ORC working fluid. The condenser was assumed at a constant temperature of 38℃. Figure 14 depicts the variation of ORC mass flow rate versus variation of turbine inlet temperature for different amounts of turbine inlet pressure. The turbine inlet temperature changed in the range of 474 K to 654 K, and turbine inlet pressure has varied between 1 MPa to 6 MPa. In these Analyses, solar radiation, inlet temperature, and flow rate of the solar working fluid were assumed equal to 800 W/m^2, 50℃, and 150 ml/s, respectively. Also, it should be mentioned that the aperture area of the investigated PTC was equal to 2 × 0.5 m^2 (see Table 1 for more detail). As seen in Figure 14, the ORC mass flow rate has reduced with increasing turbine inlet temperature. Similar results had been reported in Ref. [39]. Also, higher amounts of turbine inlet pressure have resulted in higher amounts of the ORC mass flow rate.

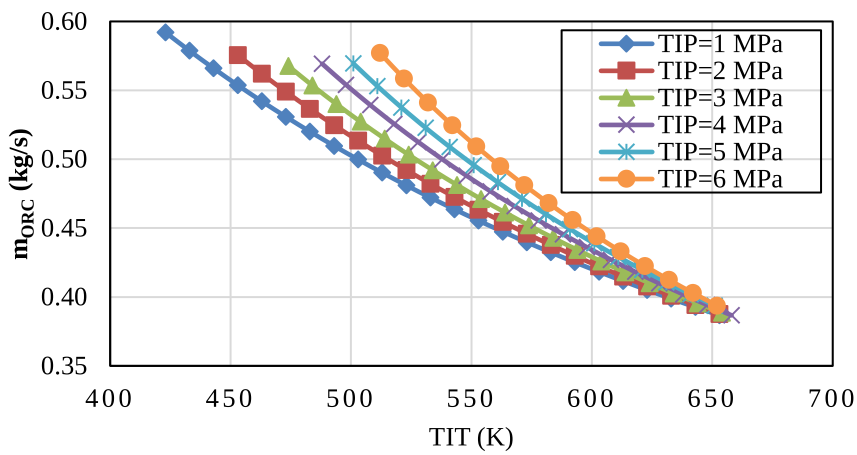

Figure 14: Variation of ORC mass flow rate versus variation of turbine inlet temperature (TIT) for different amounts of turbine inlet pressure (TIP).

Variation of ORC net work versus variation of turbine inlet temperature for different amounts of turbine inlet pressure is presented in Figure 15. It should be mentioned that the V-Shape cavity receiver with thermal oil was used as the ORC heat source. Also, ethanol was investigated as the ORC working fluid. The ORC system was considered at constant condenser temperature as 38℃. Turbine inlet temperature varied between 474 K to 654 K, and turbine inlet pressure changed between 1 MPa to 6 MPa. About the solar heat source of the ORC system, constant conditions were assumed including the solar radiation equal to 800 W/m^2, inlet temperature equal to 50℃, and flow rate of the solar working fluid as 150 ml/s. Also, it should be mentioned that the aperture area of the investigated PTC was equal to 2 × 0.5 m^2 (see Table 1 for more detail).As resulted from Figure 15, a higher amount of turbine inlet pressure, higher ORC net work. Also, there is an optimum amount of turbine inlet temperature for achieving the highest amount of the ORC net work at each level of the investigated turbine inlet pressure, as seen in Figure 15. These optimum values have occurred due to ethanol as the investigated ORC working fluid is accounted as a wet organic fluid. So, the performance of the ORC system increased with increasing TIT until ethanol remained at the two-phase condition at the inlet of the condenser. After that, with changing the phase of ethanol at the inlet of the condenser to superheat condition, then the performance of the ORC system decreased with increasing TIT. Consequently, the highest performance of the ORC system had occurred at the saturated state of ethanol at the inlet of the condenser at the constant condenser pressure. A similar conclusion has been reported in Ref. [40]. Optimum values of turbine inlet temperature and maximum ORC net work at different amounts of turbine inlet pressure have reported in Table 2. As resulted from Table 2, the maximum values of the ORC net work had increased with increasing turbine inlet pressure in the range of 170 W to 222 W. As a new finding, the highest amount of the ORC net work of the solar ORC system with the V-shape linear cavity receiver to deliver heat to the ORC system was calculated equal to 222 W at TIT of 592 K, and TIP equal to 6 MPa.

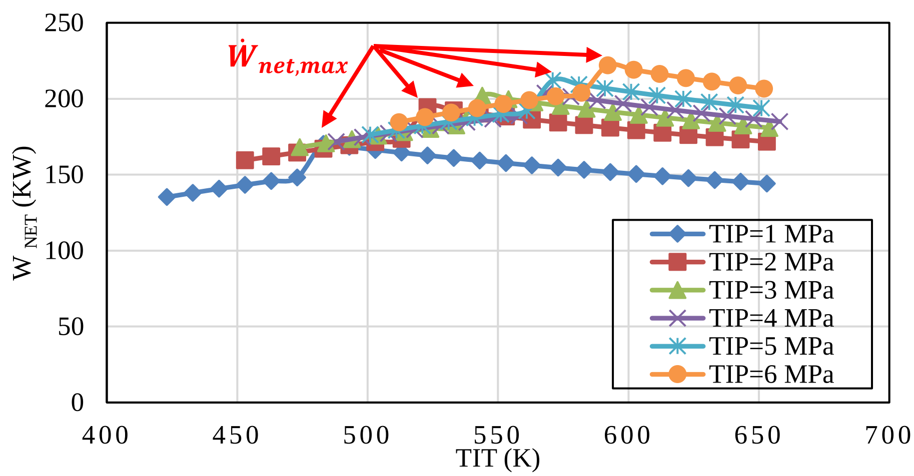

Figure 15: Variation of ORC net work versus variation of turbine inlet temperature (TIT) for different amounts of turbine inlet pressure (TIP).

Table 2: Optimum values of turbine inlet temperature, and maximum performance parameters of the solar ORC system at different turbine inlet pressures.

TIP (MPa)	1	2	3	4	5	6
TIT_{opt}(K)	483	523	544	568	571	592
W_{net} (W)	170.31	194.53	202.10	203.76	212.13	221.92
η_{ORC}	0.27	0.31	0.32	0.33	0.34	0.35
η_{total}	0.19	0.22	0.23	0.23	0.24	0.25

Figure 16 shows the variation of ORC efficiency versus variation of turbine inlet temperature in the range of 474 K to 654 K. The ORC efficiency was calculated for different levels of turbine inlet pressure between 1 MPa to 6 MPa. The solar PTC system with the linear V-Shape cavity receiver was used as the ORC heat source with the constant condition including the solar radiation equal to 800 W/m^2, inlet temperature equal to 50℃, and flow rate of the solar working fluid as 150 ml/s. Also, it should be noted that the aperture area of the investigated PTC was equal to 2 × 0.5 m^2 (see Table 1 for more detail).On the other side, thermal oil was used as the solar working fluid. It should be mentioned that ethanol was investigated as the ORC working fluid. A condenser with a constant temperature of 38℃ was used for rejecting heat from the ORC system to the ambient. In Figure 16, the ORC efficiency revealed a similar trend compared to the ORC net work tend data with vitiation of TIT, and TIP of the ORC system. In other words, the ORC efficiency improved with increasing TIP. Also, there is a maximum ORC efficiency for each investigated level of the TIP, as reported in Table 2. A new finding,the maximum ORC efficiencies with the V-shape linear cavity receiver to deliver heat to the ORC system were varied in the range of 27% to 35%. Whereas the highest ORC efficiency was calculated equal to 35% for TIT equal to 592 K, and TIP equal to 6 MPa. On the other hand, the variation of total efficiency versus variation of turbine inlet temperature for different amounts of turbine inlet pressure is depicted in Figure 17. Similar results can be explained for variation of total efficiency with changing TIT, and TIP. In other words, the higher amount of the TIP had resulted in a higher amount of total efficiency. Also, there is a maximum amount of the total efficiency for each level of the TIP, as shown in Figure 17 and reported in Table 2. A similar conclusion has been reported in Ref. [40]. As new findings, the maximum values of total efficiency of the solar ORC system with the V-shape linear cavity receiver to deliver heat to the ORC system were varied in the range of 19% to 25% with a variation of TIT, and TIP. The highest total efficiency was calculated equal to 25% for TIT equal to 592 K, and TIP equal to 6 MPa.

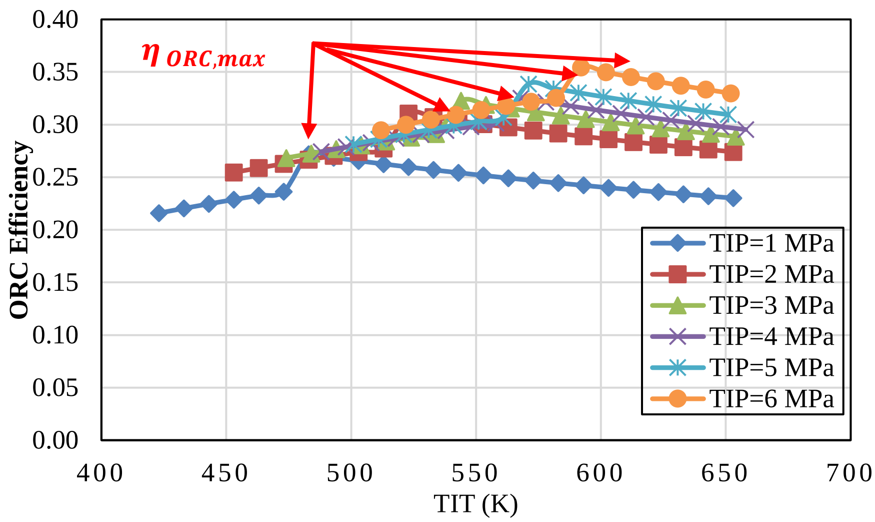

Figure 16: Variation of ORC efficiency versus variation of turbine inlet temperature (TIT) for different amounts of turbine inlet pressure (TIP).

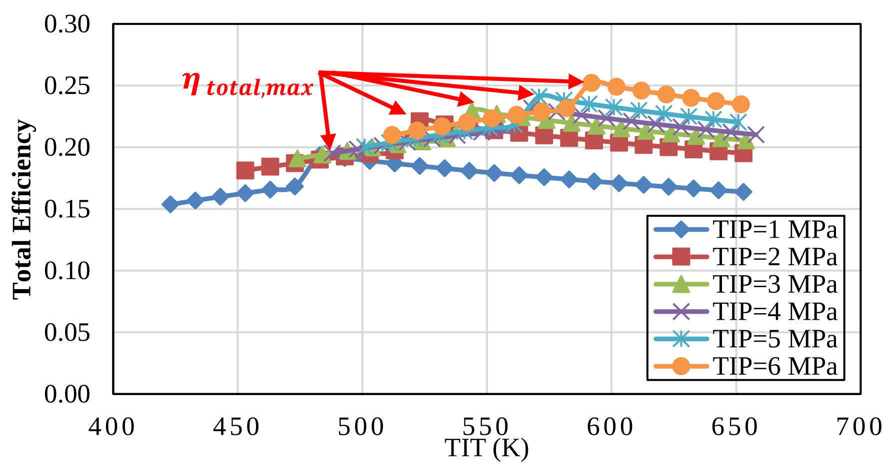

Figure 17: Variation of total efficiency versus variation of turbine inlet temperature (TIT) for different amounts of turbine inlet pressure (TIP).

Also, the variation of ORC net work versus variation of turbine inlet temperature for different amounts of the solar radiation, and inlet temperature of the solar working fluid are presented in Figure 18a, and 18b, respectively. It should be mentioned that Ethanol was used as the ORC working fluid. The ORC system was investigated at constant evaporator pressure of 3 MPa, and constant condenser temperature of 38℃. In Figure 18a, the solar radiation was varied in the range of 600 W/m^2 to 1100 W/m^2. Inlet temperature and flow rate of the solar working fluid were assumed as 50℃, and 50 ml/s, respectively. Also, it should be mentioned that the aperture area of the investigated PTC was equal to 2×0.5 m^2 (see Table 1 for more detail). As seen in Figure 18a, higher solar radiation had resulted in higher amounts of the ORC net work. About Figure 18b, the inlet temperature of solar working fluid was varied in the range of 50℃, to 240℃. Also, the reported results in Figure 18b are based on solar radiation equal to 800 W/m^2, and the flow rate of the solar working fluid equal to 50 ml/s. As seen, the lower inlet temperature of the solar working fluid resulted in higher ORC net work. Consequently, the ORC net work increased with increasing solar radiation and decreasing the inlet temperature of the solar working fluid. Similar results had been concluded in Ref. [41]. As seen, there is an optimum TIT for each level of investigated solar radiation equal to544 K. Also, a similar result has been reported in Ref. [40]. These optimum values were occurred due to ethanol as the ORC working fluid is a wet organic fluid. So, the performance of the ORC system increased with increasing TIT until the condition of ethanol at the inlet of the condenser remained in two-phase condition at constant condenser pressure. After that, phase of ethanol at the inlet of the condenser changed to superheat state and performance of the ORC system reduced with increasing TIT. Consequently, the highest performance of the ORC system had occurred at the saturated condition of ethanol at the inlet of the condenser at the constant condenser pressure. As a new finding, the ORC net work of the suggested solar ORC system with the V-shape linear cavity receiver was calculated equal to 277.87 W for the solar radiation of 1100 W/m^2. The highest amount of the ORC net work with the variation of inlet temperature was calculated equal to 201.98 W for the solar working fluid of 50 ºC. It can be seen that the solar radiation can be introduced as a more effective parameter for increasing the ORC net work compared to the inlet temperature of the solar working fluid.

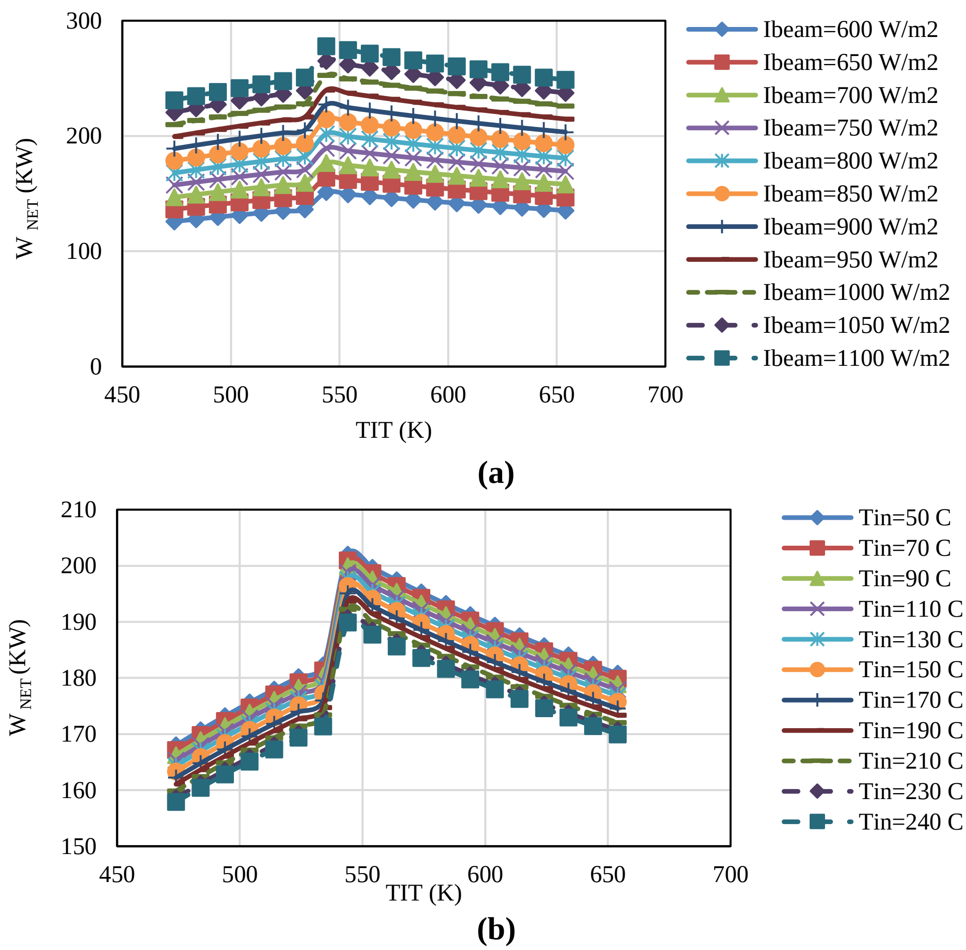

Figure 18: Variation of ORC net work versus variation of turbine inlet temperature (TIT) for different amounts of a) solar radiation, and b) inlet temperature of the solar working fluid.

Finally, Figure 19a and 19b depict the variation of total efficiency of the solar ORC system versus changes of turbine inlet temperature for different amounts of the solar radiation, and inlet temperature of the solar working fluid, respectively. It should be mentioned that the ORC system was investigated at constant evaporator pressure equal to 3 MPa, and constant condenser temperature as 38℃. Also, Ethanol was used as the ORC working fluid. Figure 19a was calculated for the solar radiation between 600 W/m^2 to 1100 W/m^2, a constant inlet temperature of 50℃, and constant flow rate of the solar working fluid equal to 50 ml/s. As displayed in Figure 19a, the total efficiency improved with increasing solar radiation. In Figure 19b, the total efficiency was calculated for the inlet temperature of the solar working fluid in the range of 50℃ to 240℃, solar radiation equal to 800 W/m^2, and the flow rate of the solar working fluid as 50 ml/s. As depicted, the total efficiency increased with decreasing inlet temperature of the solar working fluid.

Consequently, a higher amount of solar working fluid and a lower amount of the inlet temperature resulted in the higher total efficiency of the solar ORC system.As a new result, the highesttotal efficiency of the suggested solar ORC system with the V-shape linear cavity receiver to deliver heat to the ORC system was calculated equal to 31.58% for the solar radiation of 1100 W/m^2. Also, the highest amount of the total efficiency with the variation of inlet temperature was estimatedequal to 22.95% for the solar working fluid of 50 ºC. As seen, similar to the concluded results for the ORC net work, the solar radiation had a more effective parameter for increasing the total efficiency compared to the inlet temperature of the solar working fluid.

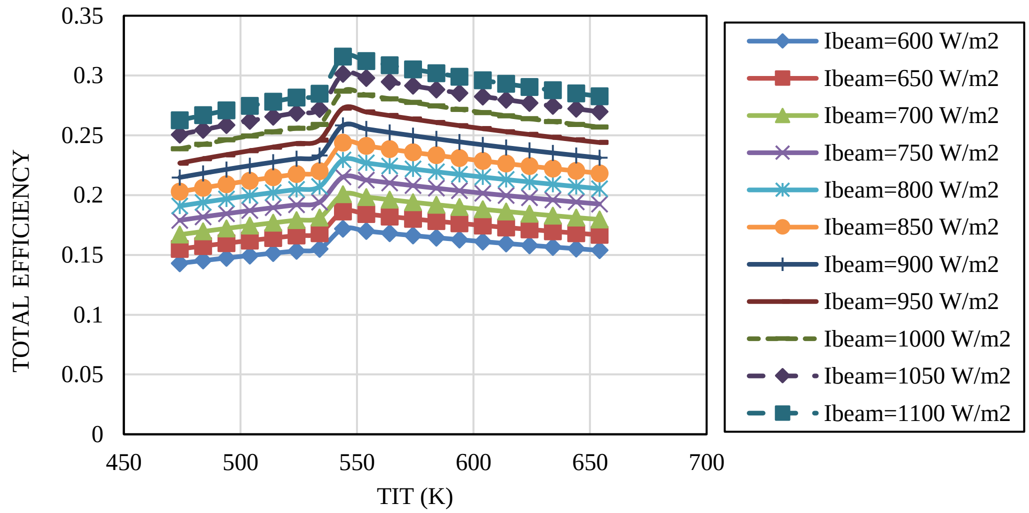

(a)

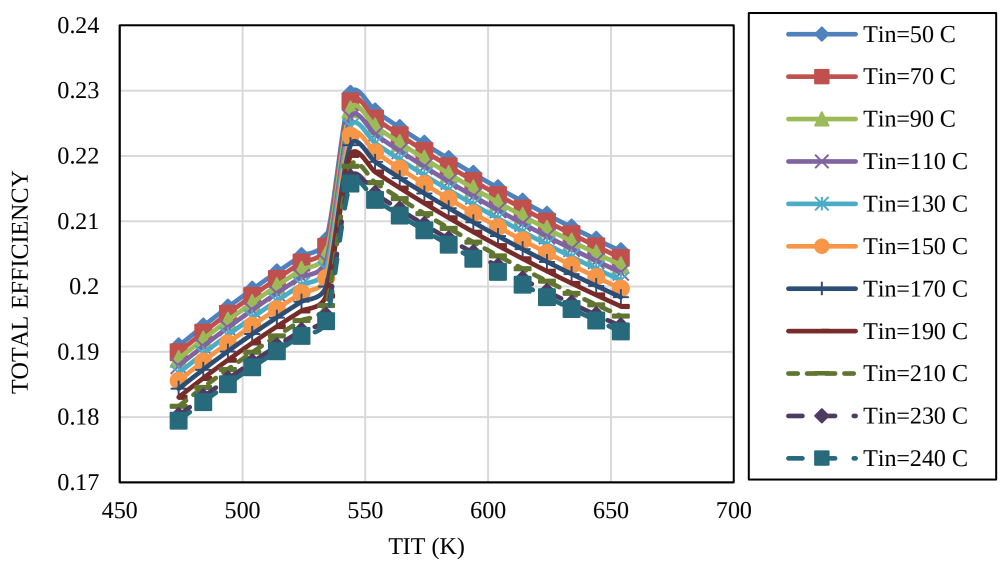

(b)

Figure 19: Variation of total efficiency of the solar ORC system versus variation of turbine inlet temperature (TIT) for different amounts of a) solar radiation, and b) inlet temperature of the solar working fluid.

3.3 Economic Analyses

In this section, economic analyses of the investigated solar ORC system for power generation are presented. The solar PTC system with the linear V-Shape cavity receiver was used as the ORC heat source with the constant condition including the solar radiation equal to 800 W/m^2, inlet temperature equal to 50℃, and flow rate of the solar working fluid as 150 ml/s. Thermal oil was used as the solar working fluid. Also, the ORC system was investigated under the condition of a constant evaporator pressure of 3 MPa, and constant condenser temperature 38℃with Ethanol as the working fluid. It should be mentioned that 100 units of the investigated solar ORC system were economically studied as a solar farm in this section of research. Variation of generated power and cash flow of the solar ORC system versus changes of turbine inlet temperature at the TIP of 3 MPa are presented in Figure 20a, and 20b, respectively. The cash flow was reported for large and small scale setups. The turbine inlet temperature was changed in the range of 474 K to 654 K. In Figure 20, there is an optimum value of turbine inlet temperature for producing the highest amounts of the power generation and cash flow. The optimum TIT was calculated as 544 K. It can be seen that the large scale setup had shown higher values of the cash flow compared to the small one. As a new result, the highest amounts of generated power and cash flow were calculated equal to 50.524 MWh, and 10044€/kWh for the large scale setup, respectively.

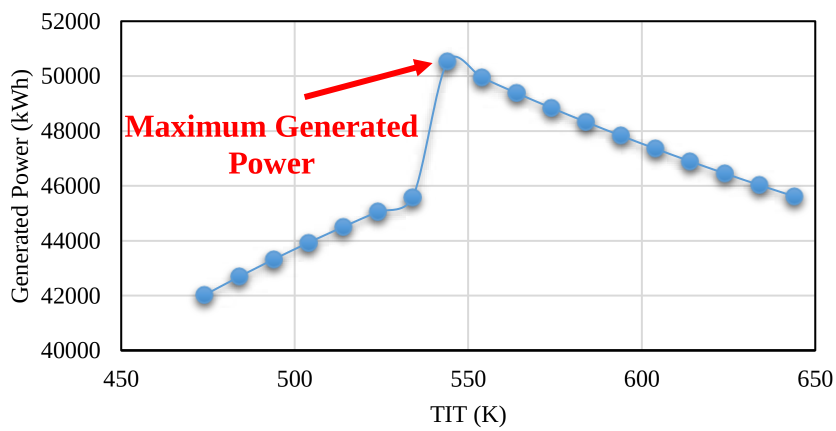

(a)

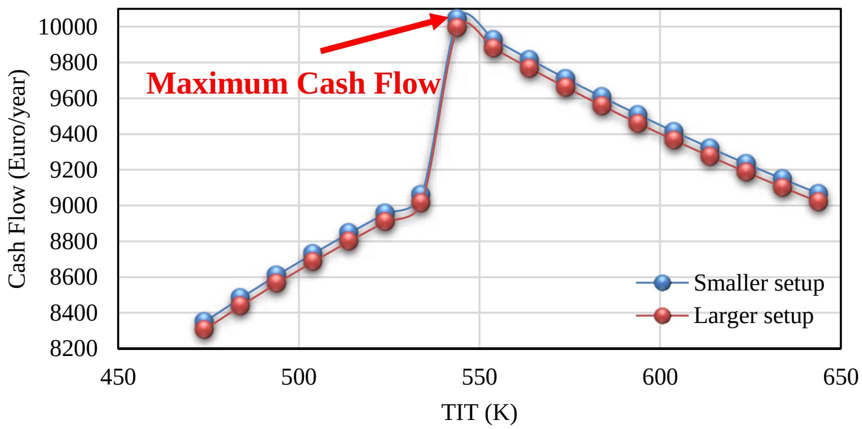

(b)

Figure 20: Variation of a) generated power, and b) cash flow of the solar ORC system versus variation of turbine inlet temperature at the TIP of 3 MPa.

The variation of LCOE and the simple payback period of the solar ORC system versus changes of turbine inlet temperature at the TIP of 3 MPa are presented in Figure 21a, and 21b, respectively. The economic analysis developed for the solar ORC system with the linear V-Shape cavity receiver was used as the ORC heat source at constant condition including the solar radiation equal to 800 W/m^2, inlet temperature equal to 50℃, and flow rate of the solar working fluid as 150 ml/s. Also, thermal oil and ethanol were used as the solar, and ORC working fluids, respectively. On the other side, the ORC evaporator, and ORC condenser were assumed at constant pressure equal to 3 MPa, and constant temperature of 38℃, respectively. As mentioned, in this section of the study, 100 units of the investigated solar ORC system were economically examined as a solar farm. The turbine inlet temperature was varied from 474 K to 654 K. In Figure 21, there is an optimum value of turbine inlet temperature equal to 544 K for achieving the lowest amounts of the LCOE and simple payback period. The LCOE was calculated for large and small scale setups.It can be seen that the large scale setup had resulted in lower amounts of the LCOE compared to the small one.As a new finding, the lowest amount of LCOE of the solar ORC system with the V-shape linear cavity receiver to deliver heat to the ORC system was calculated as 0.049€/kWh for the large scale setup, and the lowest payback period was estimated equal to 6.01 years for the large scale setup, too.

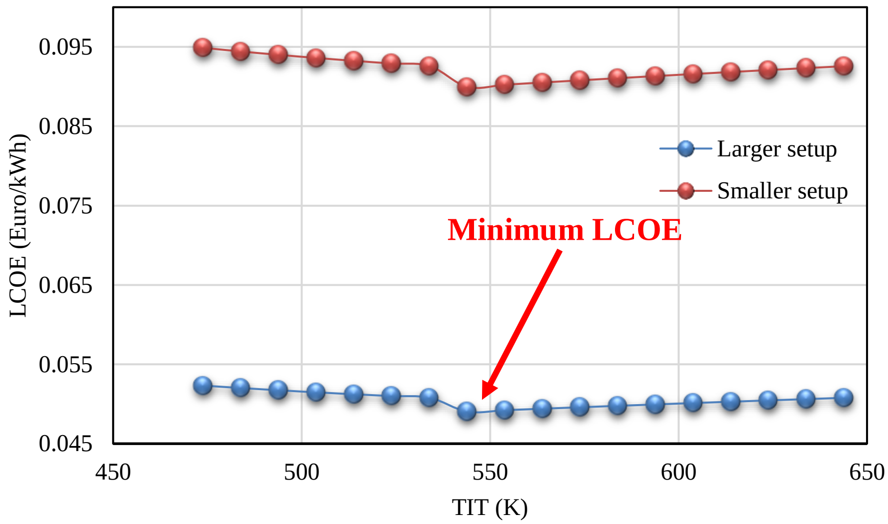

(a)

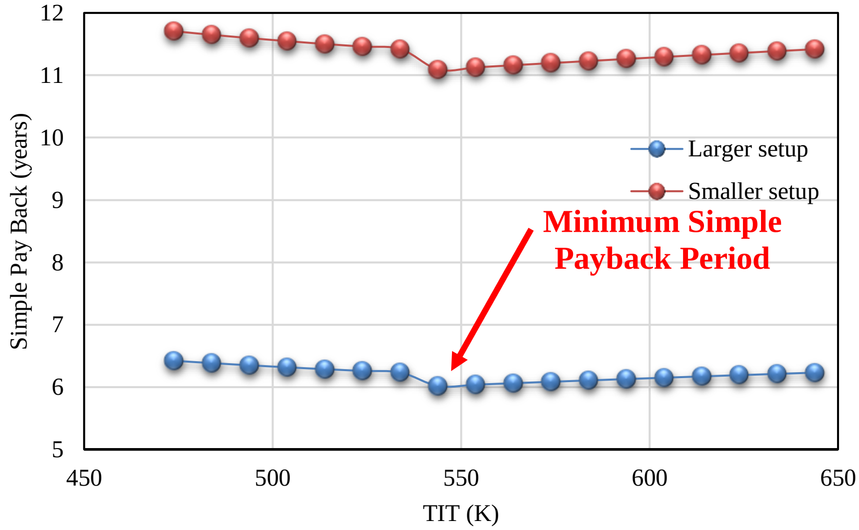

(b)

Figure 21: Variation of a) LCOE, and b) simple payback period of the solar ORC system versus variation of turbine inlet temperature at the TIP of 3 MPa.

Finally, a comparison between the calculated results in the current research with reported results by other researchers is presented in Table 3. In the current study, the maximum total efficiency of the solar ORC system using a V-shape linear cavity receiver was calculated as 25%.

It could be understood from Table 3, the calculated total efficiency of the solar ORC system had shown higher amounts compared to reported results by other researchers. It should be mentioned that the investigated PTC systems by all of the mentioned study in Table 3 are based on conventional PTC with evacuated receiver tube. As seen, Quoilin et al. [42] reported total efficiency equal to 7-8% for a solar ORC system with conventional PTC system to deliver heat to the ORC system that is lower than the calculated overall efficiency in the current research. Al-Sulaiman et al. [43] had reported total efficiency of a solar ORC system with conventional PTC system equal to 7%. In another study, Al-Sulaiman et al. [44] presented maximum electrical efficiency of a solar ORC system with conventional PTC equal to 15%. So, the examined solar ORC seems to be a highly efficient system which can compete with the other systems and so it can be used in real future applications due to its satisfactory performance.

It has to be said that the examined V-shape cavity receiver has important advantages in low and medium temperature levels compared to the conventional PTC. More specifically, the examined PTC has a relatively lower cost than the conventional PTC due to the non-utilization of the expensive evacuated tube. Moreover, the present system has higher reliability due to there is no danger of losing the vacuum in the evacuated tube. The drawback of this system is the relatively low performance in extremely high temperatures because in these cases, the thermal losses of the cavity are higher than the evacuated tube. Thus, this work suggests the utilization of the V-shape cavity with an application which has not demanded of extremely high-temperature levels.

Table 3: Comparison of the calculated results in the current research with reported results by other researchers.

Authors	Brief title	Highlights	Ref.
Quoilin et al. (2011)	A low-cost SORC for power generation with PTC	The overall efficiency of the ORC run by PTC was 7-8%.	[42]
Al-Sulaiman et al. (2011)	Modelling of a solar ORC system with PTC	The total electrical-exergy efficiency of ORC system with only solar energy, both solar energy and thermal energy storage, and with only thermal energy storage were calculated as 7%, 3.5%, and 3%, respectively.	[43]
Al-Sulaiman et al. (2011)	Solar ORC system using PTC system	The maximum electrical efficiency for the solar system appeared to be around 15% for the solar mode.	[44]
Roy et al. (2011)	Performance analysis of an solar ORC with PTC system	R-123 as the ORC unit working fluid yielded the maximum efficiencies, some 19% at 470 K Turbine Inlet Temperature.	[45]
Delgado-Torres and García-Rodríguez (2007)	Solar ORC system with PTC	The total efficiency of the system was calculated as 22.3%, 19.3%, and 18.3% using toluene, D4 and MM as the ORC working fluid, respectively.	[46]
Casati et al. (2013)	Thermal energy storage for solar-powered ORC engines with PTC collectors	A design value of the solar-to-electric efficiency was estimated 18% for the 100 kW_E solar ORC with direct thermal storage.	[47]
Bellos and Tzivanidis (2017)	A solar ORC system using PTC	Toluene was reported to be the most efficient working fluid exergetically with 29.42%; the electricity production was 177.6 kW_{el}, while the cooling and the heating production were 398.8 kW and 974.2 kW respectively.	[48]
Al-Nimr et al. (2017)	A combined CPV/T and ORC solar power system with PTC	The overall efficiency of the suggested power system could increase by 15.72%-17.78% in comparison with that of the CPV without a waste heat recovery system.	[49]
Patil et al. (2017)	Comparison of SORC and PV systems with PTC	SORC with thermal storage could be considered more reliable although its LCOE is 0.07 USD/kWh more than PV.	[50]

4 Conclusions

In this research, a solar ORC system was investigated under exergy and economic aspects. A solar PTC system with a linear V-Shape cavity receiver was used as the ORC heat source. Thermal oil and ethanol were used as the solar, and ORC working fluids, respectively. Influence of different parameters of the solar system was investigated on exergy performance of the system, including solar radiation, the inlet temperature of the solar working fluid, and flow rate of the solar working fluid. Also, the effect of some ORC parameters, including TIT and TIP, were studied on the performance of the solar ORC system and economic performance of the system. The main achievements of the current research can be summarized as follows:

- Exergy gain and exergy efficiency of the solar system had increased with increasing solar radiation, increasing the inlet temperature of the solar working fluid, and decreasing the flow rate of the solar working fluid.
- It was found that a higher amount of turbine inlet pressure, higher ORC net work. Also, there is an optimum amount of turbine inlet temperature for achieving the highest amount of the ORC net work at each level of the investigated turbine inlet pressure. The highest amount of the ORC net work was calculated equal to 222 W at TIT equal to 592 K, and TIP equal to 6 MPa.
- The ORC efficiency and total efficiency revealed a similar trend compared to the ORC net work tend data with vitiation of TIT, and TIP of the ORC system. Also, there is a maximum ORC efficiency and total efficiency for each investigated level of the TIP. The highest ORC efficiency and total efficiency were calculated equal to 35%, and 25% for TIT equal to 592 K, and TIP equal to 6 MPa, respectively.
- It was concluded that there is an optimum value of the turbine inlet temperature as 544 K for producing the highest amounts of the power generation and cash flow. The highest amounts of generated power and cash flow were calculated equal to 50.524 MWh, and 10044€/kWh for the large scale setup, respectively.
- Finally, it was found that there is an optimum value for turbine inlet temperature equal to 544 K for achieving the lowest amounts of the LCOE and the lowest simple payback period. The lowest amount of LCOE was calculated as 0.049 €/kWh for the large scale setup, and the lowest payback period was estimated equal to 6.01 years for the large scale setup.

Acknowledgment

Authors are grateful to the University of Mohaghegh Ardabili (UMA), and the Tarbiat Modares University (http://www.modares.ac.ir) for financial supports given under IG/39705 grant for renewable Energies of Modares research group.

Appendix A: Thermal Resistance Calculation

All of the mentioned thermal resistances in Figure 6 had been calculated in detail as below:

- Convection heat losses from glass cover to ambient can be calculated as following [24]:

$$R_1 = \frac{1}{A_{gc} h_{con,glass}} \tag{A-1}$$

Where

$$h_{con,glass} = \frac{0.27 \lambda_a (Gr \cdot \mathrm{Pr})^{1/4}}{d_{gc}}, d_{gc} = w_{ap} \tag{A-2}$$

$$Gr = {g \alpha \Delta T d_{gc}}^3 \big/ \nu^2 \tag{A-3}$$

- Radiation heat losses from glass cover to ambient can be assumed as below [24]:

$$R_2 = \frac{1}{A_{gc} h_{rad,glass}} \tag{A-4}$$

Where

$$\dot{Q}_{rad,glass} = \delta \varepsilon_{gc} A_{gc} \left(T_{gc}^4 - T_\infty^4\right) \tag{A-5}$$

- Internal convection heat losses to glass cover were calculated using Eq. **Error! Reference source not found.**[24]:

$$R_3 = \frac{1}{A_{cavity} h_{conv,int}} \tag{A-6}$$

Where

$$h_{conv,int} = \frac{0.59 \lambda_a (Gr \cdot \mathrm{Pr})^{1/4}}{d_0}, d_0 = cavity\ depth \tag{A-7}$$

$$Gr = {g \alpha \Delta T {d_0}^3}\Big/{\nu^2} \tag{A-8}$$

- Internal radiation heat losses to glass cover were assumed as Eq. **Error! Reference source not found.**[24]:

$$R_4 = \frac{1}{A_{cavity} h_{rad,int}} \tag{A-9}$$

Where

$$\dot{Q}_{rad,int} = \delta \varepsilon_{r-gc} A_{cavity} \left(T_s^4 - T_{gc}^4\right) \tag{A-10}$$

$$\varepsilon_{r-gc} = 1\Big/\left(\frac{1}{\varepsilon_h} + \frac{A_h}{A_{gc}} . \frac{1}{\varepsilon_{gc}} - 1\right), \quad \varepsilon_{gc} = 0.95, and\ \varepsilon_h = 0.05 \tag{A-11}$$

- Conduction heat losses from insulation layer can be calculated as following [32]:

$$R_5 = \frac{t_{ins}}{k_{ins} A_{cavity}} \tag{A-12}$$

As seen from Figure 5, outer sides of the linear V-Shape cavity receiver were covered using insulation for reducing heat losses. Mineral wool with a thickness of 2 cm and an average insulation conductivity of 0.062 W/mK [51], was used as the insulation.

- Radiation heat losses from the insulation layer to ambient was assumed as below [32]:

$$R_6 = \frac{1}{A_{cavity} h_{rad,ext}} \tag{A-13}$$

Where

$$\dot{Q}_{rad,ext} = \delta \varepsilon A_{cavity} \left(T_s^4 - T_\infty^4\right) \tag{A-14}$$

- Convection heat losses from the insulation layer to ambient was calculated as Eq. **Error! Reference source not found.**[32].

$$R_6 = \frac{1}{A_{cavity} h_{con,ext}} \tag{A-15}$$

Based on the thermal resistance method, total internal heat losses can be calculated as below [32]:

$$\dot{Q}_{loss,int} = \frac{T_s - T_{amb}}{R_{total,int}} \tag{A-16}$$

Where

$$R_{total,int} = \frac{R_1 R_2}{R_1 + R_2} + \frac{R_3 R_4}{R_3 + R_4} \tag{A-17}$$

On the other side, the total external heat losses can be calculated as following [32]:

$$\dot{Q}_{loss,int} = \frac{T_s - T_{amb}}{R_{total,ext}} \tag{A-18}$$

Where

$$R_{total,ext} = R_5 + \frac{R_6 R_7}{R_6 + R_7} \tag{A-19}$$

Finally, total resistance heat losses can be calculated based on the following equation [32]:

$$R_{total} = R_{total,int} + R_{total,ext} \tag{A-20}$$

References

[1] J.M.K. Atte Harjanne, Abandoning the concept of renewable energy, Energy Policy, 127 (2019) 330-340.

[2] A. Mohammadi, M. Mehrpooya, A comprehensive review on coupling different types of electrolyzer to renewable energy sources, Energy, (2018).

[3] E. Bellos, C. Tzivanidis, Assessment of linear solar concentrating technologies for Greek climate, Energy conversion and management, 171 (2018) 1502-1513.

[4] J. Qin, E. Hu, G.J. Nathan, L. Chen, Concentrating or non-concentrating solar collectors for solar Aided Power Generation?, Energy Conversion and Management, 152 (2017) 281-290.

[5] H.G. Massaab El Ydrissi, El Ghali Bennouna, Abdi Farid Geometric, optical and thermal analysis for solar parabolic trough concentrator efficiency improvement using the Photogrammetry technique under semi-arid climate, (2019).

[6] E. Bellos, C. Tzivanidis, Alternative designs of parabolic trough solar collectors, Progress in Energy and Combustion Science, 71 (2019) 81-117.

[7] S. Pavlovic, R. Loni, E. Bellos, D. Vasiljević, G. Najafi, A. Kasaeian, Comparative study of spiral and conical cavity receivers for a solar dish collector, Energy Conversion and Management, 178 (2018) 111-122.

[8] K. Mansour, R. Boudries, R. Dizene, Optical, 2D thermal modeling and exergy analysis applied for performance prediction of a solar PTC, Solar Energy, 174 (2018) 1169-1184.

[9] L.S. Conrado, A. Rodriguez-Pulido, G. Calderón, Thermal performance of parabolic trough solar collectors, Renewable and Sustainable Energy Reviews, 67 (2017) 1345-1359.

[10] Q. Chen, Z. Yuan, Z. Guo, Y. Zhao, Practical performance of a small PTC solar heating system in winter, Solar Energy, 179 (2019) 119-127.

[11] B. Lamrani, A. Khouya, B. Zeghmati, A. Draoui, Mathematical modeling and numerical simulation of a parabolic trough collector: A case study in thermal engineering, Thermal Science and Engineering Progress, 8 (2018) 47-54.

[12] T. Moudakkar, Z. ElHallaoui, S. Vaudreuil, T. Bounahmidi, Modeling and performance analysis of a PTC for industrial phosphate flash drying, Energy, (2018).

[13] M. Fathy, H. Hassan, M.S. Ahmed, Experimental study on the effect of coupling parabolic trough collector with double slope solar still on its performance, Solar Energy, 163 (2018) 54-61.

[14] F. Razmmand, R. Mehdipour, S.M. Mousavi, A Numerical Investigation on the Effect of Nanofluids on Heat Transfer of the Solar Parabolic Trough Collectors, Applied Thermal Engineering, (2019).

[15] M.A. Rehan, M. Ali, N.A. Sheikh, M.S. Khalil, G.Q. Chaudhary, T. ur Rashid, M. Shehryar, Experimental performance analysis of low concentration ratio solar parabolic trough collectors with nanofluids in winter conditions, Renewable Energy, 118 (2018) 742-751.

[16] M. Potenza, M. Milanese, G. Colangelo, A. de Risi, Experimental investigation of transparent parabolic trough collector based on gas-phase nanofluid, Applied Energy, 203 (2017) 560-570.

[17] E. Bellos, C. Tzivanidis, D. Tsimpoukis, Enhancing the performance of parabolic trough collectors using nanofluids and turbulators, Renewable and Sustainable Energy Reviews, 91 (2018) 358-375.

[18] R. Bader, M. Barbato, A. Pedretti, A. Steinfeld, An air-based cavity-receiver for solar trough concentrators, Journal of Solar Energy Engineering, 132 (2010) 031017.

[19] A.M. Daabo, S. Mahmoud, R.K. Al-Dadah, The effect of receiver geometry on the optical performance of a small-scale solar cavity receiver for parabolic dish applications, Energy, 114 (2016) 513-525.

[20] R. Loni, E.A. Asli-Ardeh, B. Ghobadian, A. Kasaeian, S. Gorjian, Numerical and experimental investigation of wind effect on a hemispherical cavity receiver, Applied Thermal Engineering, 126 (2017) 179-193.

[21] R. Loni, A.B. Kasaeian, E.A. Asli-Ardeh, B. Ghobadian, S. Gorjian, Experimental and Numerical Study on Dish Concentrator with Cubical and Cylindrical Cavity Receivers using Thermal Oil, Energy, (2018).

[22] P.L. Singh, R. Sarviya, J. Bhagoria, Thermal performance of linear Fresnel reflecting solar concentrator with trapezoidal cavity absorbers, Applied Energy, 87 (2010) 541-550.

[23] Y. Qiu, Y.-L. He, M. Wu, Z.-J. Zheng, A comprehensive model for optical and thermal characterization of a linear Fresnel solar reflector with a trapezoidal cavity receiver, Renewable Energy, 97 (2016) 129-144.

[24] X. Xiao, P. Zhang, D. Shao, M. Li, Experimental and numerical heat transfer analysis of a V-cavity absorber for linear parabolic trough solar collector, Energy conversion and management, 86 (2014) 49-59.

[25] A.M. Delgado-Torres, L. García-Rodríguez, Analysis and optimization of the low-temperature solar organic Rankine cycle (ORC), Energy Conversion and Management, 51 (2010) 2846-2856.

[26] M. Wang, J. Wang, Y. Zhao, P. Zhao, Y. Dai, Thermodynamic analysis and optimization of a solar-driven regenerative organic Rankine cycle (ORC) based on flat-plate solar collectors, Applied Thermal Engineering, 50 (2013) 816-825.

[27] C. Tzivanidis, E. Bellos, K.A. Antonopoulos, Energetic and financial investigation of a stand-alone solar-thermal Organic Rankine Cycle power plant, Energy conversion and Management, 126 (2016) 421-433.

[28] E. Bellos, C. Tzivanidis, C. Symeou, K.A. Antonopoulos, Energetic, exergetic and financial evaluation of a solar driven absorption chiller–A dynamic approach, Energy conversion and management, 137 (2017) 34-48.

[29] A. Najafi, A. Jafarian, J. Darand, Thermo-economic evaluation of a hybrid solar-conventional energy supply in a zero liquid discharge wastewater treatment plant, Energy Conversion and Management, 188 (2019) 276-295.

[30] W.G. Le Roux, T. Bello-Ochende, J.P. Meyer, The efficiency of an open-cavity tubular solar receiver for a small-scale solar thermal Brayton cycle, Energy Conversion and Management, 84 (2014) 457-470.

[31] R. Loni, A. Kasaeian, E.A. Asli-Ardeh, B. Ghobadian, Optimizing the efficiency of a solar receiver with tubular cylindrical cavity for a solar-powered organic Rankine cycle, Energy, 112 (2016) 1259-1272.

[32] Y.A. Cengel, A.J. Ghajar, M. Kanoglu, Heat and mass transfer: fundamentals & applications, McGraw-Hill New York, 2011.

[33] R. Loni, A. Kasaeian, E.A. Asli-Ardeh, B. Ghobadian, W. Le Roux, Performance study of a solar-assisted organic Rankine cycle using a dish-mounted rectangular-cavity tubular solar receiver, Applied Thermal Engineering, 108 (2016) 1298-1309.

[34] Y.A. Cengel, ThermodynamicsAn Engineering Approach 5th Edition By Yunus A Cengel: ThermodynamicsAn Engineering Approach, Digital Designs, 2011.

[35] A. Kasaeian, S. Daviran, R.D. Azarian, A. Rashidi, Performance evaluation and nanofluid using capability study of a solar parabolic trough collector, Energy conversion and management, 89 (2015) 368-375.

[36] R. Loni, A. Kasaeian, O. Mahian, A.Z. Sahin, S. Wongwises, Exergy analysis of a solar organic Rankine cycle with square prismatic cavity receiver, International Journal of Exergy, 22 (2017) 103-124.

[37] R. Loni, S. Pavlovic, E. Bellos, C. Tzivanidis, E.A. Asli-Ardeh, Thermal and exergy performance of a nanofluid-based solar dish collector with spiral cavity receiver, Applied Thermal Engineering, 135 (2018) 206-217.

[38] R. Loni, E.A. Asli-Ardeh, B. Ghobadian, E. Bellos, W.G. Le Roux, Numerical comparison of a solar dish concentrator with different cavity receivers and working fluids, Journal of Cleaner Production, 198 (2018) 1013-1030.

[39] R. Loni, A. Kasaeian, O. Mahian, A. Sahin, Thermodynamic analysis of an organic rankine cycle using a tubular solar cavity receiver, Energy Conversion and Management, 127 (2016) 494-503.

[40] K. Shahverdi, R. Loni, B. Ghobadian, M. Monem, S. Gohari, S. Marofi, G. Najafi, Energy harvesting using solar ORC system and Archimedes Screw Turbine (AST) combination with different refrigerant working fluids, Energy Conversion and Management, 187 (2019) 205-220.

[41] (!!! INVALID CITATION !!!).

[42] S. Quoilin, M. Orosz, H. Hemond, V. Lemort, Performance and design optimization of a low-cost solar organic Rankine cycle for remote power generation, Solar energy, 85 (2011) 955-966.

[43] F.A. Al-Sulaiman, I. Dincer, F. Hamdullahpur, Exergy modeling of a new solar driven trigeneration system, Solar Energy, 85 (2011) 2228-2243.

[44] F.A. Al-Sulaiman, F. Hamdullahpur, I. Dincer, Performance comparison of three trigeneration systems using organic rankine cycles, Energy, 36 (2011) 5741-5754.

[45] J. Roy, M. Mishra, A. Misra, Performance analysis of an Organic Rankine Cycle with superheating under different heat source temperature conditions, Applied Energy, 88 (2011) 2995-3004.

[46] A.M. Delgado-Torres, L. García-Rodríguez, Comparison of solar technologies for driving a desalination system by means of an organic Rankine cycle, Desalination, 216 (2007) 276-291.

[47] E. Casati, A. Galli, P. Colonna, Thermal energy storage for solar-powered organic Rankine cycle engines, Solar energy, 96 (2013) 205-219.

[48] E. Bellos, C. Tzivanidis, Parametric analysis and optimization of a solar driven trigeneration system based on ORC and absorption heat pump, Journal of Cleaner Production, 161 (2017) 493-509.

[49] A.-N. Moh'd A, M. Bukhari, M. Mansour, A combined CPV/T and ORC solar power generation system integrated with geothermal cooling and electrolyser/fuel cell storage unit, Energy, 133 (2017) 513-524.

[50] V.R. Patil, V.I. Biradar, R. Shreyas, P. Garg, M.S. Orosz, N. Thirumalai, Techno-economic comparison of solar organic Rankine cycle (ORC) and photovoltaic (PV) systems with energy storage, Renewable Energy, 113 (2017) 1250-1260.

[51] S. Melcome, K. Khanlari, A. Mouradian, A. Ajemian, N. Ohan, Technical Information, Pashme Sang Iran, Engineering and Design Department, (2002).